UNIVERSITÉ DU QUÉBEC À MONTRÉAL

ASSEMBLAGES DE FORAMINIFÈRES BENTHIQUES DU CHENAL LAURENTIEN DE L'ESTUAIRE MARITIME ET DU GOLFE DU SAINT-LAURENT, EST DU CANADA : TRACEURS D'HYPOXIE DES EAUX DE FOND

MÉMOIRE

PRÉSENTÉ

COMME EXIGENCE PARTIELLE

DE LA MAÎTRISE EN SCIENCES DE LA TERRE

PAR

TIFFANY AUDET

MARS 2023

UNIVERSITÉ DU QUÉBEC À MONTRÉAL
Service des bibliothèques

Avertissement

REMERCIEMENTS

AVANT-PROPOS

Ce mémoire de maîtrise est présenté sous la forme d'un article scientifique qui a été soumis à la revue *Journal of Foraminiferal Research* le 18 août 2022 et publié le 20 janvier 2023 après modifications majeures. Par conséquent, la mise en forme et l'utilisation de la langue anglaise respectent les exigences de la revue et non celles de l'Université du Québec à Montréal.

TABLE DES MATIÈRES

LISTE DES FIGURES

LISTE DES TABLEAUX

LISTE DES ABRÉVIATIONS, DES SIGLES ET DES ACRONYMES

aff.   *Affiliate*

Affilié

ca.   *Circa*

Environ

cal   *Calibrated years*

Années calibrées

CE   *Common Era*

Ère commune

cf.   *Confer*

Se reporter à

CF (CRS)   *Constant flux (Constant Rate of Supply)*

Flux constant (Taux d'apports constant)

CL   Chenal Laurentien

CIL   *Cold Intermediate Layer*

Couche froide intermédiaire

C_{org} *Organic carbon*

Carbone organique

e.g.   *Exempli gratia*

Par exemple

EMSL	Estuaire maritime du Saint-Laurent
GSL	*Gulf of St. Lawrence*
	Golfe du Saint-Laurent
IC	*Inorganic carbon*
	Carbone inorganique
i.e.	*Id est*
	C'est-à-dire
LC	*Laurentian Channel*
	Chenal laurentien
LCW	*Labrador Current Water*
	Courant des eaux du Labrador
LSLE	*Lower St. Lawrence Estuary*
	Estuaire maritime du Saint-Laurent
NACW	*North Atlantic Central Water*
	Courant des eaux centrales nord-atlantiques
N_{tot}	Azote Total
PCA	*Principal component analysis*
	Analyse en composantes principales
PC	*Principal component*
	Composante principale
R^2	Coefficient de corrélation
RDA	*Redundancy analysis*
	Analyse de redondance

SCD   *Square chord distance*

     Distance des carrés

sp.   Espèce au singulier

spp.   *Species pluralis*

     Plusieurs espèces

TC   *Total carbon*

     Carbone Total

TN   *Total nitrogen*

     Azote total

LISTE DES SYMBOLES ET DES UNITÉS

a	Année
~	Environ
%	Pourcent
‰	Pour mille
±	Plus ou moins
>	Supérieur à
≥	Supérieur ou égal à
<	Inférieur à
°	Degré
°C	Degré Celsius
'	Minute d'arc
α	Alpha (radiation)
δ	Delta
λ	Gamma (constante de désintégration)
σ	Sigma (déviation standard)
n	Nombre d'échantillons
µg	Microgramme
g	Gramme
L	Litre

mL	Millilitre
μM	Micromole
μm	Micromètre
mm	Millimètre
cm	Centimètre
m	Mètre
km	Kilomètre
meV	Milliélectronvolt
keV	Kiloélectronvolt
$[O_2]$	Concentration en oxygène dissous
s	Seconde
S_P	*Practical salinity*
	Salinité
$t_{1/2}$	Demi-vie
T	Température
X	Fois

RÉSUMÉ

Au cours du dernier siècle, une augmentation des températures et une diminution des concentrations en oxygène dissous ont été observées dans les eaux de fond du chenal Laurentien (CL), dans l'estuaire maritime (EMSL) et dans l'ouest du Golfe du Saint-Laurent (GSL), dans l'est du Canada. Afin de documenter l'impact de ces changements, nous avons analysé les assemblages de foraminifères benthiques et la composition géochimique de quatre carottes de sédiments prélevées dans le CL. Les mesures radiométriques (^{210}Pb, ^{226}Ra, ^{137}Cs) indiquent que les carottes étudiées couvrent les 50 dernières années dans l'EMSL et les ~160 dernières années dans le GSL. L'enregistrement sédimentaire révèle une diminution de 60 à 65 % de la diversité taxonomique des foraminifères benthiques dans le CL depuis les années 1960. Une évolution accélérée des assemblages de foraminifères est observée approximativement au même moment dans toutes les stations étudiées, vers la fin des années 1990 et le début des années 2000, vers des populations dominées par les taxons indicateurs, tolérants à l'hypoxie : *Brizalina subaenariensis*, *Eubuliminella exilis* et *Globobulimina auriculata*. Cette évolution des assemblages reflète les incursions de la zone hypoxique dans l'ouest du GSL au cours des dernières décennies. Les résultats des analyses multivariées mettent en évidence le potentiel des assemblages de foraminifères benthiques comme proxy de l'hypoxie des eaux de fond.

Mots-clés : foraminifères benthiques, hypoxie, Chenal Laurentien, estuaire, golfe du Saint-Laurent, eaux de fond, environnement

INTRODUCTION GÉNÉRALE

Au cours du siècle dernier, des changements des concentrations en oxygène dissous et de la température des eaux de fond ont été mesurées ou reconstituées dans l'estuaire maritime (EMSL) et le golfe du Saint-Laurent (GSL), dans l'est du Canada (Gilbert *et al.*, 2005; Thibodeau *et al.*, 2006 ; Genovesi *et al.*, 2011 ; Jutras *et al.*, 2020a). Les mesures historiques des concentrations en oxygène dissous des eaux de fond de l'EMSL révèlent une diminution de plus de 50 %, passant de ~125 µM L^{-1} dans les années 1930 à une moyenne de ~60 (±6) µM L^{-1} entre 1985 et 2018 (Gilbert *et al.*, 2005 ; Jutras *et al.*, 2020a). Au cours des 20 dernières années, la zone hypoxique de l'EMSL s'est étendue, de façon irrégulière, de 1300 km^2 en 2002 à 9700 km^2 en 2021 (Jutras et al., 2022).

Les écosystèmes marins benthiques de l'EMSL et du GSL sont directement affectés par un appauvrissement en oxygène (Belley et al., 2010). Les effets néfastes sur le biote marin incluent une réduction de la croissance et de la reproduction des espèces marines exploitées commercialement, telles la morue et la crevette nordique (D'Amours, 1993; Chabot et Dutil, 1999; Dupont-Prinet *et al.*, 2013). De plus, une fois le niveau hypoxique atteint (<63 µM L^{-1}), les populations de poissons et les écosystèmes marins sont vulnérables aux facteurs de stress supplémentaires, naturels et anthropiques (Breitburg, 2002). Dans l'EMSL, on observe déjà des changements dans les communautés benthiques, avec une augmentation des espèces tolérantes à l'hypoxie (Gilbert *et al*., 2007; Belley *et al*., 2010).

L'appauvrissement en oxygène dissous dans les eaux profondes du chenal Laurentien (CL) a été attribué à divers facteurs, incluant les changements dans la circulation

océanique dans le Nord-ouest Atlantique (Gilbert *et al.*, 2005; Thibodeau *et al.*, 2018; Jutras *et al.*, 2020a), l'augmentation des flux de matière organique et de nutriments (c.-à-d. eutrophisation) dans l'EMSL (Thibodeau *et al.*, 2006, 2010; Jutras *et al.*, 2020a, b), ainsi qu'à l'augmentation des températures des eaux de fond qui entraîne une amplification des taux de respiration microbienne (Genovesi *et al.*, 2011). Dans une étude récente, Jutras *et al.* (2020a) ont défini que les principales causes de l'appauvrissement de l'oxygène dissous des eaux de fond du CL auraient changé au cours des 50 dernières années : l'impact de la respiration microbienne amplifiée en réponse à l'augmentation de la températures et à l'eutrophisation a probablement été déterminant entre les années 1970 et la fin des années 1990, tandis qu'une contribution plus faible des eaux froides et riches en oxygène dissous du courant du Labrador (LCW), par rapport aux eaux centrales de l'Atlantique Nord (NACW), plus chaudes et appauvries en oxygène, est invoquée pour la période entre 2008 et 2018.

Quelles que soient les causes de l'appauvrissement en oxygène dissous, la diminution de l'oxygénation des eaux de fond du chenal Laurentien au cours du siècle dernier a entraîné des variations dans les assemblages de foraminifères benthiques préservés dans les sédiments (Thibodeau *et al.*, 2006; Genovesi *et al.*, 2011). Les foraminifères benthiques sont des organismes unicellulaires vivant sur ou dans les sédiments marins, et constituent une partie de la microfaune marine. Leur partie fossilisable, le test, peut être fait de carbonate de calcium (foraminifère carbonaté) ou de particules de sables ou de détritus agglutinées par l'organisme (foraminifères agglutinants). Bien que les mécanismes physiologiques de réponse aux changements environnementaux soient encore méconnus, il est observé que certains taxons développent des affinités pour des conditions environnementales précises, alors que d'autres sont plus tolérants (Murray, 2001, 2006). Les foraminifères sont donc un outil paléoécologique fréquemment utilisé pour les reconstructions paléo-environnementales. Puisque certaines espèces de foraminifères benthiques sont sensibles aux changements d'oxygénation des eaux de fond (Sen Gupta et Machain-Castillo, 1993; Loubere, 1994; Bernhard *et al.*, 1997;

Karlsen *et al.*, 2000; Osterman, 2003; Platon *et al.*, 2005), l'abondance et la diversité des espèces peuvent être utilisées pour évaluer qualitativement et quantitativement (Ohkushi *et al*., 2013; Hoogakker *et al*., 2018; Tetard *et al*., 2017, 2021a, b; Erdem *et al*., 2020) le niveau d'oxygénation des eaux de fond. La température, la production primaire, les flux de carbone organique et la distribution des masses d'eau peuvent également moduler la distribution des assemblages (e.g., Jorissen *et al.*, 2007). Les études antérieures de Hooper (1975) et Rodrigues et Hooper (1982) fournissent un aperçu exhaustif de la distribution des foraminifères benthiques dans les sédiments prélevés dans l'EMSL et le GSL dans les années 1970. Quelques autres études documentent les changements récents dans les assemblages des foraminifères benthiques à quelques sites le long du CL dans l'EMSL (Thibodeau *et al.*, 2006, 2010) et dans le GSL (Genovesi *et al.*, 2011). Ces études ont révélé la sensibilité des foraminifères benthiques aux changements des conditions physico-chimiques des eaux de fond. Entre autres, on observe dans l'EMSL l'apparition et une rapide augmentation de l'abondance relative des espèces *Brizalina subaenariensis* et *Eubuliminella exilis* (appelée *Bulimina exilis* dans Thibodeau *et al*., 2006), deux taxons tolérants les faibles conditions d'oxygénation (Kaiho, 1994; Sen Gupta, 1999; Brüchert *et al.,* 2000), à partir des années 1960. Thibodeau *et al.* (2006) attribuent cette apparition simultanée de ces deux espèces aux phénomènes d'eutrophisation, suivant une augmentation considérable des activités agricoles et industrielles au début des années 1960. Dans le GSL, Genovesi *et al.* (2011) observent également une augmentation de *B. subaenariensis*, accompagnée d'une diminution de l'espèce *Nonionellina labradorica*, cette dernière étant une espèce indicatrice du LCW. L'évolution des assemblages de foraminifères benthiques semble ainsi révéler un réchauffement des eaux et un changement dans l'apport du LCW au GSL.

Dans la présente étude, nous analysons la composition géochimique et les assemblages de foraminifères benthiques de quatre carottes sédimentaires récupérées dans le chenal Laurentien de l'EMSL et du GSL en juin 2018 (Fig. 1.1; Table 1.1). L'enregistrement

sédimentaire couvre les dernières décennies à la station 23 et jusqu'à ~1860 à la station 16. Les deux principaux objectifs de l'étude sont : (1) de documenter comment les assemblages de foraminifères benthiques récents et sub-récents ont changé avec l'évolution temporelle et spatiale de la zone hypoxique à travers le CL, et (2) d'évaluer semi-quantitativement la relation entre la composition des assemblages de foraminifères benthiques et les concentrations en oxygène dissous des eaux de fond. Le travail inclut une description complète et systématique des assemblages de foraminifères benthiques récents et sub-récents dans le CL, ainsi que des analyses statistiques. Les hypothèses de recherche sont (1) que les assemblages de foraminifères benthiques ont évolué vers des populations de faible biodiversité, dominées par des espèces tolérantes à l'hypoxie, et ce, dans les quatre stations à l'étude, et (2) les analyses statistiques effectuées sur les assemblages des foraminifères benthiques permettront d'établir une relation empirique entre les foraminifères benthiques, du moins certaines espèces-clés, et l'oxygénation des eaux de fond.

Le choix d'une approche micropaléontologique pour aborder la problématique de l'hypoxie dans le CL repose sur son originalité. À l'heure actuelle, les projets de recherche sur l'hypoxie dans l'EMSL sont principalement menés dans une perspective biologique et chimique. Cependant, les études biologiques ne fournissent que des données sur l'état actuel ou récent de cet environnement, étant donné la courte vie des organismes vivants. La micropaléontologie est une source de données peu exploitée dans le domaine de l'environnement, mais qui a l'avantage d'apporter une dimension nouvelle et pertinente grâce aux échelles temporelles qu'elle permet d'aborder. De manière générale, les microfossiles offrent de précieuses informations sur les paramètres environnementaux, notamment par l'étude de leurs populations et par leur composition chimique et isotopique. En analysant les microfossiles et leurs assemblages, il est possible de remonter dans le temps et de retracer les conditions du passé, donc d'évaluer l'ampleur des changements environnementaux suite à des variations du climat ou un stress anthropogénique. L'étude des foraminifères

benthiques est particulièrement appropriée à la caractérisation des environnements benthiques. Ceux-ci sont de très bons traceurs de la qualité des conditions environnementales passées (Kaiho, 1994; Sen Gupta *et al.* 1993; Murray, 2006). Les résultats de ce projet sont utiles d'un point de vue méthodologique, puisqu'ils contribuent au développement d'une approche originale pour retracer quantitativement les concentrations en oxygène dissous dans le fond de l'EMSL et du GSL au cours des siècles derniers.

Un modèle d'âge pour les quatre carottes a été déterminé sur la base de la distribution verticale du plomb-210 dans les sédiments. Les résultats des analyses géochimiques et micropaléontologiques nous ont permis de reconstituer les variations temporelles des concentrations et des flux de foraminifères benthiques ainsi que de les relier aux mesures *in situ* des concentrations d'oxygène dissous dans les eaux de fond de l'EMSL entre ~1930 et 2018, établissant ainsi un traceur régional d'hypoxie.

CHAPITRE I

BENTHIC FORAMINIFERAL ASSEMBLAGES FROM THE LAURENTIAN CHANNEL IN THE LOWER ESTUARY AND GULF OF ST. LAWRENCE, EASTERN CANADA : TRACERS OF BOTTOM-WATER HYPOXIA

Tiffany Audet[1*], Anne de Vernal[1], Alfonso Mucci[2], Marit-Solveig Seidenkrantz[3], Claude Hillaire-Marcel[1], Vladislav Carnero-Bravo[4], Yves Gélinas[5]

Correspondence author. Email: audet.tiffany@courrier.uqam.ca

1 Département des Sciences de la Terre et de l'Atmosphère and Geotop-UQAM C.P. 8888, succ. Centre-ville, Montreal, Quebec, Canada H3C 3P8

2 Department of Earth & Planetary Sciences and Geotop-McGill, 3450 University St., Montreal, Quebec, Canada H3A 0E8

3 Department of Geoscience, Aarhus University, Høegh-Guldbergs Gade 2, 8000 Aarhus C, Denmark

4 Instituto de Ecología, Universidad del Mar, Campus Puerto Ángel, Puerto Ángel, Oaxaca, México

5 Geotop and Department of Chemistry & Biochemistry, Concordia University, 7141 Sherbrooke St. W. Montreal, Quebec, Canada H4B 1R6

Abstract

Over the past century, an increase in temperatures and a decrease in dissolved oxygen concentrations have been observed in the bottom waters of the Laurentian Channel (LC), throughout the Lower St. Lawrence Estuary (LSLE) and the western Gulf of St. Lawrence (GSL), eastern Canada. To document the impact of these changes, we analyzed the benthic foraminiferal assemblages and geochemical composition of four sediment cores taken in the LC. Radiometric measurements (^{210}Pb, ^{226}Ra, ^{137}Cs) indicate that the studied cores encompass the last 50 years of sedimentation in the LSLE and the last ~160 years in the GSL. The sedimentary record shows a 60 to 65% decrease in benthic foraminiferal taxonomic diversity in the LC since the 1960s. An accelerated change in the foraminiferal assemblages is observed at approximately the same time at all studied stations, around the late 1990s and the early 2000s, towards populations dominated by the hypoxia-tolerant indicator taxa *Brizalina subaenariensis*, *Eubuliminella exilis*, and *Globobulimina auriculata.* This evolution of assemblages reflects incursions of the hypoxic zone into the western GSL over the last decades. The results of our multivariate analyses highlight the potential of benthic foraminiferal assemblages as a proxy of bottom-water hypoxia.

Keywords: benthic foraminifera, hypoxia, Laurentian Channel, estuary, Gulf of St. Lawrence, bottom-water, environment

1.1   Introduction

Over the past century, changes in bottom-water oxygenation and temperatures were measured or reconstructed in the Lower St. Lawrence Estuary (LSLE) and the Gulf of St. Lawrence (GSL) in eastern Canada (Gilbert et al., 2005, 2007; Thibodeau et al., 2006; Genovesi et al., 2011; Jutras et al., 2020a). Historical measurements of dissolved oxygen (DO) concentrations in the bottom waters of the Lower St. Lawrence Estuary

(LSLE) reveal a decrease of more than 50%, from ~125 µM L^{-1} in the 1930s to an average of ~60 (±6) µM L^{-1} between 1985 and 2018 (Gilbert et al., 2005; Jutras et al., 2020a). This impacted benthic marine ecosystems (Belley et al., 2010) and has had deleterious effects on the marine biota, including reduced growth and reproduction of commercially exploited marine species such as cod and northern shrimp (D'Amours, 1993; Chabot & Dutil, 1999; Dupont-Prinet et al., 2013). Furthermore, at hypoxic levels (<62.5 µM L^{-1}), fish populations are increasingly vulnerable to additional stressors, natural and anthropogenic (Breitburg, 2002; Belley et al., 2010).

Oxygen depletion in the deep waters of the LSLE and GSL has been attributed to various factors, including changes in ocean circulation in the northwest Atlantic (Gilbert et al., 2005; Thibodeau et al., 2018; Jutras et al., 2020a), increased organic matter and nutrient fluxes (i.e., eutrophication) in the LSLE (Thibodeau et al., 2006, 2010; Jutras et al., 2020a, b) as well as increased bottom-water temperatures and the associated enhanced microbial respiration rates (Genovesi et al., 2011). In a recent study, Jutras et al. (2020a) determined that the dominant causes of oxygen depletion in the bottom waters of the LC may have changed over the last 50 years: the impact of enhanced microbial respiration in response to warmer bottom-water temperatures and eutrophication was likely determinant between the 1970s and the late 1990s, while a lower contribution of cold, oxygen-rich Labrador Current Water (LCW), relative to the warmer, oxygen-depleted North Atlantic Central Water (NACW) may be invoked between 2008 and 2018.

Regardless of the causes of oxygen depletion, the decrease in bottom-water oxygenation in the Laurentian Channel over the past century resulted in variations in the benthic foraminiferal assemblages preserved in the sediment (Thibodeau et al., 2006; Genovesi et al., 2011). As benthic foraminifera are sensitive to bottom-water oxygenation (Sen Gupta & Machain-Castillo, 1993; Loubere, 1994; Bernhard et al., 1997; Karlsen et al., 2000; Osterman, 2003; Platon et al., 2005), the abundance and

diversity of species can be used to qualitatively and quantitatively (Ohkushi et al., 2013; Hoogakker et al., 2018; Tetard et al., 2017, 2021a, b; Erdem et al., 2020) assess the level of bottom-water DO concentrations. Temperature, primary production, organic carbon fluxes, and water mass distribution may also modulate the distribution of the assemblages (e.g., Jorissen et al., 2007). Previous studies by Hooper (1975) and Rodrigues & Hooper (1982) provided a comprehensive overview of the benthic foraminiferal distribution in sediment collected in the Estuary and Gulf of St. Lawrence in the 1970s. A few other studies documented recent changes in benthic foraminiferal assemblages at a few sites along the Laurentian Channel in the LSLE (Thibodeau et al., 2006, 2010) and the GSL (Genovesi et al., 2011). These studies revealed the sensitivity of benthic foraminifera to changes in bottom-water conditions.
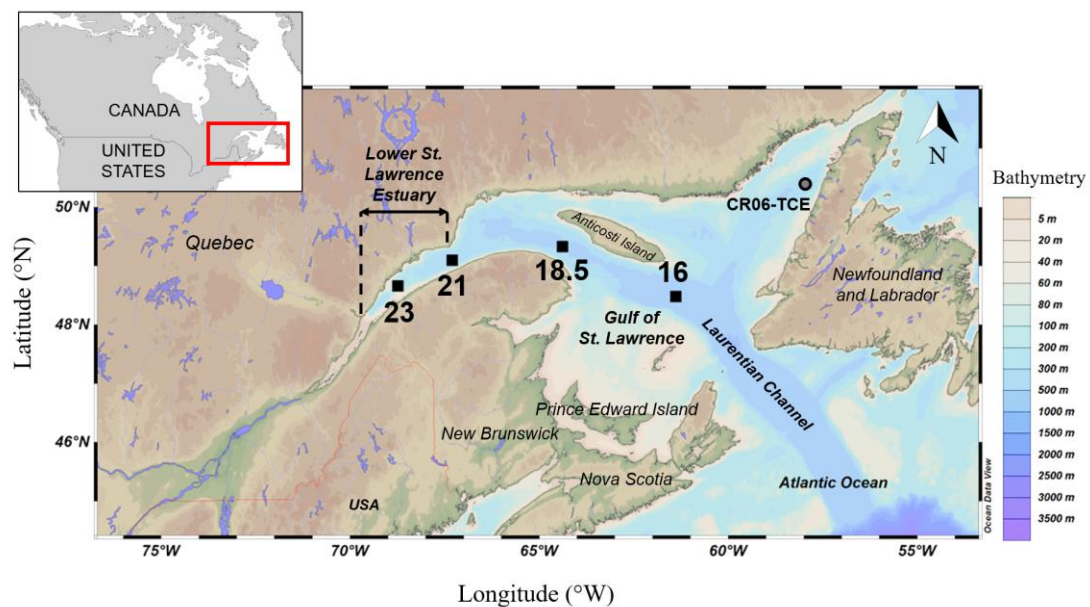
Figure 1.1   Map of the Estuary and Gulf of St. Lawrence with location of the study stations (23, 21, 18.5 and 16) in the LC (see Table 1 for precise location and bottom-water properties), as well as core CR06-TCE in the Esquiman Channel (Thibodeau et al., 2013). The cores were collected in 2018; sediment cores recovered

at station 23 in 2000 and station 16 in 2005 were, respectively, analyzed and interpreted by Thibodeau et al. (2006) and Genovesi et al. (2011).

In this study, we analyzed the geochemical composition and micropaleontological content of four sediment cores collected in June 2018 in the LC of the LSLE and GSL. The records encompass decades to a few centuries. The two main objectives were: (1) to document how the recent and sub-recent benthic foraminiferal assemblages changed with the temporal and spatial evolution of the hypoxic zone across the LC, and (2) to semi-quantitatively evaluate the rates of changes in benthic foraminiferal assemblages in relation to bottom-water oxygenation.

1.2   Study area

The St. Lawrence Estuary system on the eastern coast of Canada is considered to be the largest semi-enclosed estuary in the world (Fig. 1.1). The freshwater discharge at Quebec City is estimated at 11,000 $m^3 s^{-1}$, second only to the Mississippi in North America (Bourgault & Koutinonsky, 1999). Its main bathymetric feature is the Laurentian Channel (LC), a 300–500 m deep, U-shaped submarine valley that extends ~1280 km landward from the continental shelf break to the head of the Lower St. Lawrence Estuary (LSLE) at Tadoussac (Figs. 1.1, 1.2). The LSLE and the Gulf of St. Lawrence (GSL) are characterized by an estuarine circulation. During most of the sea ice-free season, the water column consists of a three-layer system based on its thermal stratification. The surface layer (0–30 m) flows seaward and results from the mixing of water from the northwest North Atlantic and freshwater from the St. Lawrence River and tributaries along its north shore (Dinauer & Mucci, 2018). It is characterized by relatively low salinities (S_P = ~25–31, where S_P is the practical salinity) and seasonally variable temperatures. It overlies the Cold Intermediate Layer (CIL), a cold (T = –1 to 2°C) and saline (S_P = ~32 to 33) water mass that forms in winter in the gulf and flows landward at depths between 50 and ~150 m (Gilbert & Pettigrew, 1997; Galbraith,

2006). The deep waters below ~150 m originate from a mixture of warm, oxygen-poor North Atlantic Central Water (NACW) and cold, oxygen-rich Labrador Current Water (LCW), that enter the GSL through Cabot Strait (Dickie & Trites, 1983; Gilbert et al., 2005; Fig. 1.2B). They are relatively warm (T = 4–7°C) and salty (S_P = ~33–35). In winter, cooling and decreased freshwater input result in vertical mixing of the surface layer and CIL (Galbraith, 2006; Smith et al., 2006; Saucier et al., 2009). The surface waters are in contact with the atmosphere and, thus, well-oxygenated. However, the deep waters, which are isolated from the atmosphere by the persistent stratification, progressively lose DO through microbial respiration and remineralization of organic matter during their 4 to 7–years landward journey from the continental shelf break to the head of the LC (Bugden, 1991; Gilbert, 2004; Benoit et al., 2006). Consequently, highly oxygen-depleted bottom waters are observed throughout the LSLE and the western GSL (Gilbert et al., 2005; Jutras et al., 2020a, 2022). Any change in the ocean circulation that modifies the relative contributions of the LCW and NACW to the bottom waters of the LC, in addition to variations in organic matter fluxes and temperature, may play a role in modulating oxygenation conditions in the LSLE and GSL.

12
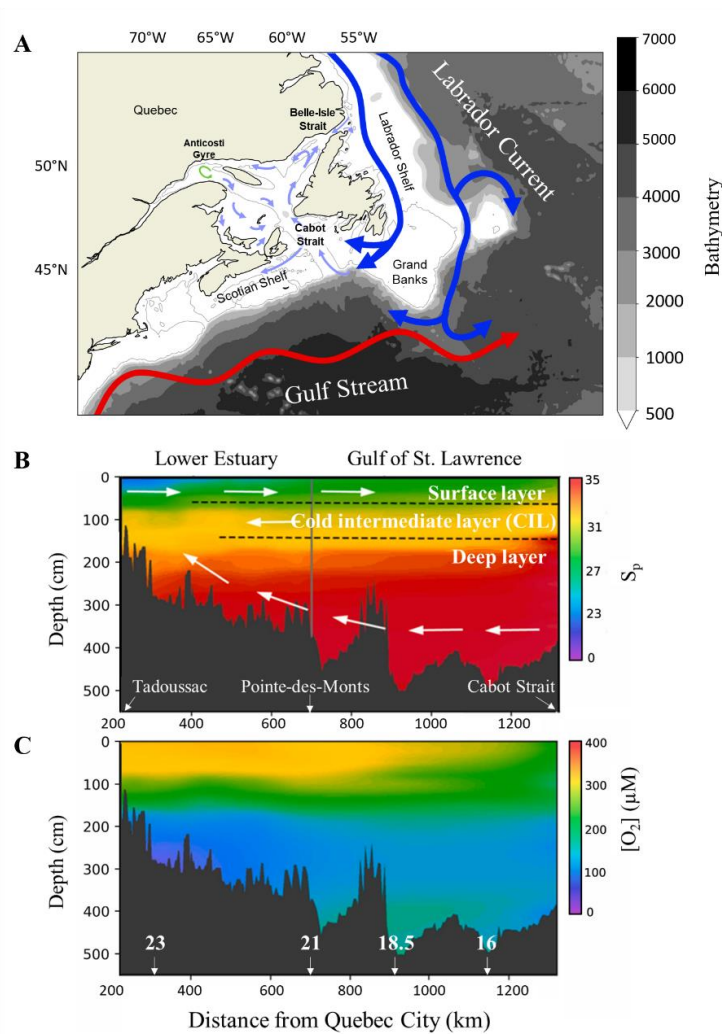
Figure 1.2   A) Map of the main currents of the St. Lawrence Estuary and Gulf. The arrows represent the approximate position of: the Labrador Current in dark blue; the Gulf Stream in red; the Anticosti Gyre in green; the inner currents of the Gulf in light blue. B) Schematic representation of the summer three-layer stratification along the Laurentian Channel. Colors represent practical salinity. C) Dissolved oxygen concentrations and approximate locations of stations 23, 21, 18.5 and 16 along the Laurentian Channel. Data extracted in 2020 from the BioChem database made available by the Department of Fisheries and Oceans Canada. Modified after Jutras et al. (2020b).

1.3   Materials and methods

1.3.1   Coring sites and sampling

Four sediment cores were recovered in the LSLE and GSL in June 2018 aboard the *R/V Coriolis II* (Fig. 1.1; Table 1.1) using an Ocean Instrument Mark II box corer. Each box core (0.12 m^2 x 0.5 m high) was transferred to a specially designed stainless-steel glove box (Edenborn et al., 1987) for subsampling. Stations 23, 21, 18.5, and 16, at which the box cores were recovered, are part of a network of recurring stations along the LC that have been visited regularly over the past 40 years. Each core was subsampled at 0.5 cm increments for the first cm. Core from station 23 was subsampled at 1 cm increments from 1 to 5 cm, 2 cm increments from 5 to 15 cm, and 3 or 4 cm increments to the bottom of the cores. Cores from stations 21, 18.5 and 16 were subsampled at 1 cm increments to the bottom of the cores. At each depth interval, sediment samples were transferred and stored in two pre-weighed plastic vials. One set of vials was later weighed, freeze-dried, and weighed again to determine the water content. Sediment porosity was calculated from the water content, the salinity of the overlying seawater, and a dry sediment density of 2.65 g cm^{-3}. The freeze-dried sediments were then ground and homogenized with an agate pestle and mortar in preparation for later analyses (e.g., organic carbon). A known volume (6 to 8 mL) of a Rose Bengal solution (2 g L^{-1} in ethanol, density = 0.79 g mL^{-1}) was added to each of another set of vials to stain the living foraminifera. All subsamples we analyzed were stained, except for those below 25 cm from station 23. These vials were subsequently weighed, and the sediment porosity was used to determine the dry-sediment weight. The exact location, water depth, overlying water salinity, and DO concentrations at each sampling station are reported in Table 1.1.

14

Table 1.1   Location of the core sites and bottom-water properties (practical salinity and dissolved oxygen) measured during sampling.

Station	Latitude (N)	Longitude (W)	Water depth (m)	Bottom-water practical salinity	Bottom-water dissolved oxygen concentration (μM)	Core length (cm)	Analysed core length (cm)
23	48°40.15'	–68°44.25'	340	34.52	56.2	41	41
21	49°05.00'	–67°18.15'	325	34.46	58.2	20	13
18.5	49°19.50'	–64°23.30'	389	34.78	77.0	20	15
16	48°29.80'	–61°24.70'	418	34.93	117.0	20	20

1.3.2   Core chronology and sedimentation rates

The chronological framework was established from ^{210}Pb measurements for all study cores, and from both ^{210}Pb and ^{137}Cs measurements for station 23. The ^{210}Pb activity in sediment was obtained indirectly by measuring the decay rate of its daughter isotope ^{210}Po ($t_{1/2}$ = 138.4 days; α = 5.30 MeV) by alpha spectrometry assuming secular equilibrium. Following the protocol proposed by Flynn (1968), ^{209}Po was added to the freeze-dried samples as a spike to determine the extraction and counting efficiency and to measure the decay rate. The samples were submitted to a series of acid digestions (HCl, HNO$_3$, HF, and H$_2$O$_2$) and the purified polonium was chemically deposited on a silver disk. The $^{209-210}$Po activities were measured in a silicon surface-barrier multichannel α-spectrometer (EGG-ORTEC, type 576A) coupled to a MAESTRO Multichannel Analyzer Emulation Software. Uncertainties were estimated from counting statistics to be approximately 6% for two standard deviations (2σ).

Sedimentation rates were estimated using the ^{210}Pb-decay constant (λ), the linear least-squares regression slope of the logarithmic function of excess ^{210}Pb and the CF (CRS) model with Monte Carlo uncertainty under the assumption of a constant rate of supply.

The *Plum* software (Aquino-López et al., 2018) under R (R Core Team, 2021) was used to define the age models for each core (Fig. 1.3), taking into consideration the total ($^{210}Pb_{tot}$) and supported ($^{210}Pb_{sup}$) ^{210}Pb activities, the density (g cm^{-3}) of samples, and the coring date.

The $^{210}Pb_{sup}$ was determined in the bottom section of the cores using the activity of the parent isotope ^{226}Ra. To confirm the validity of the chronological framework, we measured the vertical distribution of ^{137}Cs activity in the sediment core recovered from station 23. The ^{137}Cs activity was measured at 661.6 keV and the ^{226}Ra activity was measured at 295.22, 352, and 609.32 keV using a Canberra low-background high-purity Ge well-detector. The reproducibility of ^{226}Ra and ^{137}Cs activity measurements was estimated at ± 1% (1σ) based on replicate analyses ($n = 6$) of the Columbia River Basalt reference material (BCR-2; USGS).

1.3.3   Sedimentary carbon and nitrogen analyses

Total carbon (C_{tot}) and total nitrogen (N_{tot}) content of the freeze-dried, ground, and homogenized sediment samples were determined using a Carlo Erba^{TM} NC 2500 elemental analyzer (NC2500TM) at the Geotop Research Center. The inorganic carbon (IC) content of the sediments was determined independently using a UIC coulometer, following acidification of a weighed aliquot of the freeze-dried samples and CO_2 extraction. The precision of this analysis is better than ±2%. The organic carbon content (C_{org}) was obtained from the difference between C_{tot} and IC ($C_{org} = C_{tot} - IC$). The standard deviation (1σ) on the C_{tot} and N_{tot} analyses was estimated at, respectively, 0.1% and 0.3%, based on replicate measurements of organic analytical standard substances (acetanilide, atropine, cyclohexanone-2,4-dinitrophenyl-hydrazone, and urea).

For isotopic analyses of C_{org}, freeze-dried, ground and homogenized sediment samples were fumed in a desiccator for 48 hours in the presence of concentrated hydrochloric acid to dissolve carbonate phases. The isotopic composition of C_{org} ($\delta^{13}C_{org}$) was measured with a Micromass Isoprime[TM] ratio mass spectrometer in-line with an Elementar Vario MicroCube[TM] elemental analyzer in continuous flow mode. Data are reported in the δ notation in ‰ with respect to V-PDB (Coplen, 1995) (Fig. 1.4). As determined from replicate measurements of standard materials, the analytical uncertainty was estimated at $\pm$ 0.1‰. To normalize the results on the NBS19-LSVEC scale, two internal reference materials ($\delta^{13}C = -28.73 \pm 0.06$‰ and $\delta^{13}C = -11.85 \pm 0.04$‰) were used, and a third reference material ($\delta^{13}C = -17.04 \pm 0.11$‰) was analyzed as an unknown to assess the accuracy of the normalization.

1.3.4   Benthic foraminiferal analyses

Each sediment sample was treated according to the procedure described by de Vernal et al. (1999). Depending on the liquid content of the subsamples, 5 to 13 cm^3 of wet sediment were weighed, dried at room temperature, weighed again, and wet-sieved through 63 µm and 106 µm mesh sieves. Both these fractions were examined under a binocular microscope at 40X and 100X magnification. Calcareous and agglutinated benthic foraminifera were hand-sorted, enumerated, identified, and counted according to the nomenclature of Rodrigues (1980) and Loeblich & Tappan (1987). Planktonic foraminifera were not counted, as they only occurred occasionally. Well-preserved specimens of calcareous benthic foraminifera, photographed using a Keyence[TM] microscope, are presented in Figures A1 and A2. The list of all observed taxa and their relative abundance (e.g., rare, occasional, common) in the LSLE and GSL sediments are reported in Table A1.

To evaluate the relevance of using the >63 µm fraction, which can contain small size tests and juvenile forms often difficult to identify, benthic foraminifera from station 16

were wet-sieved both at 106 μm and 63 μm. Analysis of the 63–106 μm fraction revealed the presence of additional species, compared to the >106 μm fraction, including *Pullenia osloensis*, *Alabaminella weddellensis*, *Bolivinellina pseudopunctata*, *Nonionoides turgidus, Stainforthia fusiformis*, *Bolivina* aff. *alata*, and *Valvulineria arctica* as well as species from the Polymorphinidae family and the genera *Fissurina* and *Parafissurina*. Considering the significantly higher species richness in the >63 μm fraction compared to the >106 μm fraction, we choose to systematically analyze the >63 μm. The detailed foraminiferal counts, with distinction of tests stained with Rose Bengal and the proportion of small (<106 µm) tests, can be found in Tables A2 and A3.

In this study, we present the occurrence of all identified benthic foraminiferal species. We report the total concentration including both tests stained with Rose Bengal and non-stained specimens. In oxygen-depleted environments, the protoplasm of dead foraminifera may be preserved for several months (Bernhard, 1988; Corliss & Emerson, 1990) and staining by the Rose Bengal can lead to an overestimation of the abundance of living individuals at greater depths (Fontanier et al., 2002; Bernhard et al., 2006). Hence, we applied strict staining criteria, as described in Fontanier et al. (2002), to overcome the inaccuracies of the method at greater depths, by counting individuals as living only if the Rose Bengal stained all chambers except the last one. Partly stained tests were still noted as an indicator of the presence of an undecayed protoplasm.

The relative abundance of various taxa, expressed as percentages, were calculated for all taxa but only common and occasional taxa are reported. The relative abundance of taxa that accounts for ≥3% of the assemblages in at least one sample per core are presented in Figure 1.5.

Multivariate analyses using the CANOCO 5 software (ter Braak & Šmilauer, 2012) were conducted with the percentages of calcareous taxa to help define zonation and

assemblages. We performed principal component analyses (PCA) and illustrated the scores of the two main principal components (first axis PC1; and second axis, PC2) on ordination diagrams available in the Supplementary Materials. We also performed a constrained redundancy analysis (RDA) based on the calcareous assemblage at station 23, and the temperature and DO as environmental variables. Finally, we calculated dissimilarity coefficients using the squared chord distance (SCD) to define the depth of the most pronounced changes in assemblages (Overpeck et al., 1985). In the studies of Woodroffe (2009) and Benito et al. (2015), the SCD method was applied to compare samples with modern analogues, and the largest dissimilarity coefficient were used as critical thresholds to define dissimilar assemblages. Following this approach, we used the highest SCD value in each core as the critical threshold to define transitions. The PCA, RDA, and multivariate SCD analyses were conducted on taxa that accounts for ≥3% of the assemblage in at least one sample to reduce crowding and the effect of rare taxa on the analyses.

1.4   Results

1.4.1   Excess ^{210}Pb, ^{137}Cs activities and sedimentation rates

Uniform values of the excess ^{210}Pb activity (^{210}Pb$_{ex}$) in the upper part of the cores are interpreted as delimiting the depth of the mixed layer (Fig. 1.3). At station 23, the ln(^{210}Pb$_{ex}$) data can be fit to a simple linear equation with a slope of -0.05 ($R^2 = 0.98$), corresponding to a sedimentation rate of ~0.70 ± 0.03 cm a^{-1}. At station 21, the linear fit to the ln(^{210}Pb$_{ex}$) data yields a slope of -0.08 ($R^2 = 0.96$), corresponding to a sedimentation rate of ~0.42 ± 0.03 cm a^{-1} (Fig. 1.3B). At station 18.5, the linear fit to the ln(^{210}Pb$_{ex}$) data yields a slope of -0.12 ($R^2 = 0.96$), corresponding to a sedimentation rate of ~0.27 ± 0.03 cm a^{-1} (Fig. 1.3C). At station 16, the results suggests that there may have been a change in sedimentation rates. The slope to the data in the upper 5 cm

is -0.10 ($R^2 = 0.96$), corresponding to a sedimentation rate of $\sim 0.31 \pm 0.03$ cm a^{-1}. The slope to the data in the 5−20 cm interval is -0.04 ($R^2 = 0.97$), corresponding to a sedimentation rate of $\sim 0.11 \pm 0.03$ cm a^{-1} (Fig. 1.3D). Based on ^{210}Pb and ^{137}Cs measurements, Genovesi et al. (2011) also concluded that sedimentation rates in this area of the GSL may have varied through time over the previous two centuries. The sedimentation rates obtained in this study are consistent with estimates from Thibodeau et al. (2006) at station 23 and Genovesi et al. (2011) near station 16.

We assume a constant flux of ^{210}Pb to set a chronology. Our chronological framework, established with the *Plum* model, was confirmed by measurements of ^{137}Cs activities throughout the core recovered at station 23. Assuming that the location of the ^{137}Cs peak at a sub-bottom depth of ~ 25 cm (not shown) corresponds to 1986 CE, the year of the Chernobyl incident, our ^{210}Pb-based age model at this station is accurate. Furthermore, the correlation of the benthic foraminiferal species *Brizalina subaenariensis* and *Eubuliminella exilis* between our station 23 core and core CR02-23 investigated by Thibodeau et al. (2006), taken at the same location, indicates that the bottom of our core (41 cm) is not older than ~ 1960, as the two species first appeared around this time in CR020-23.

According to our age models and the above-mentioned correlation, we estimate that the cores we recovered from station 23 encompass the last ~ 50 years of sedimentation (i.e., ~ 1965–2018 CE). Thus, the geochemical and micropaleontological analyses performed at 0.5– and 1–cm intervals provide time series with sub-annual to decadal resolution. The *Plum* settings and output for each station are available in the Supplementary Materials (Fig. S1).

A Station 23

$^{210}Pb_{tot}$ & ^{226}Ra (Bq kg^{-1})   Ln(^{210}Pb excess)

Mixed layer

Depth (cm)

^{137}Cs peak ~ 1986

Sedimentation rate ~ 0.7 cm a^{-1}, R^2 = 0.98

- ● ^{210}Pb activity
- ■ ^{226}Ra activity
- ---- Estimate of the supported ^{210}Pb fraction
- — Best linear fit of the ln ^{210}Pb data below mixed layer

B Station 21

$^{210}Pb_{tot}$ & ^{226}Ra (Bq kg^{-1})   Ln(^{210}Pb excess)

Mixed layer

Depth (cm)

Sedimentation rate ~ 0.4 cm a^{-1}, R^2 = 0.90

C Station 18.5

$^{210}Pb_{tot}$ & ^{226}Ra (Bq kg^{-1})   Ln(^{210}Pb excess)

Mixed layer

Depth (cm)

Sedimentation rate ~ 0.3 cm a^{-1}, R^2 = 0.96

D Station 16

$^{210}Pb_{tot}$ & ^{226}Ra (Bq kg^{-1})   Ln(^{210}Pb excess)

Mixed layer?

Depth (cm)

Sedimentation rate ~ 0.3 cm a^{-1}, R^2 = 0.96

Change in sedimentation rate ~ 0.1 cm a^{-1}, R^2 = 0.97

Figure 1.3   Excess lead-210 (ln) at A) station 23, B) station 21, C) station 18.5, and D) station 16 (core locations in Table 1.1 and Fig. 1.1). The red circles represent the ^{210}Pb data. The blue circles represent the ^{226}Ra data from which the supported ^{210}Pb value (vertical dotted line) was estimated. At stations 21 and 18.5, the supported ^{210}Pb was estimated from data at the bottom section of the cores. The depth of the mixed layer (highlighted in grey) and/or sediment density change is not taken into consideration in the sedimentation rate calculation. Sedimentation rates were calculated from the linear regression below the mixed layer.

1.4.2   Geochemistry of sedimentary organic matter

The organic carbon content (w/w) of the sediment in the four study cores ranges from 1.26% to 1.91%. There is a slight increase in organic carbon content from the LSLE to the GSL, with an average of 1.55% at station 23, 1.53% at station 21, 1.61% at station 18.5, and 1.75% at station 16. However, these values do not necessarily equate to higher organic carbon fluxes and productivity. They may reflect a lower dilution by organic material inputs of terrestrial origin, as would suggest the $\delta^{13}C_{org}$ data. The organic carbon fluxes can be computed based on the estimated sedimentation rates (Fig. 1.4). The average total mass accumulation rates are 1.54, 0.99, 0.68 and 0.25 g cm^{-2} a^{-1} at stations 23, 21, 18.5 and 16, respectively.

The organic carbon content of all four cores typically decreases slightly with depth, while the $C_{org}:N_{tot}$ molar ratio increases slightly (Fig. 1.4). This may be attributed to the preferential degradation of nitrogen-rich organic matter during early diagenesis (Meyers, 1997; Muzuka & Hillaire-Marcel, 1999).

The $\delta^{13}C_{org}$ data show distinct signatures at each study site, with lower values in the LSLE and higher values in the GSL. The mean $\delta^{13}C_{org}$ are –24.2‰ at station 23, –23.2‰ at station 21, –22.6‰ at station 18.5, and –22.1‰ at station 16. They reflect the higher proportions of terrestrial versus marine organic matter at stations in the LSLE than in the GSL.
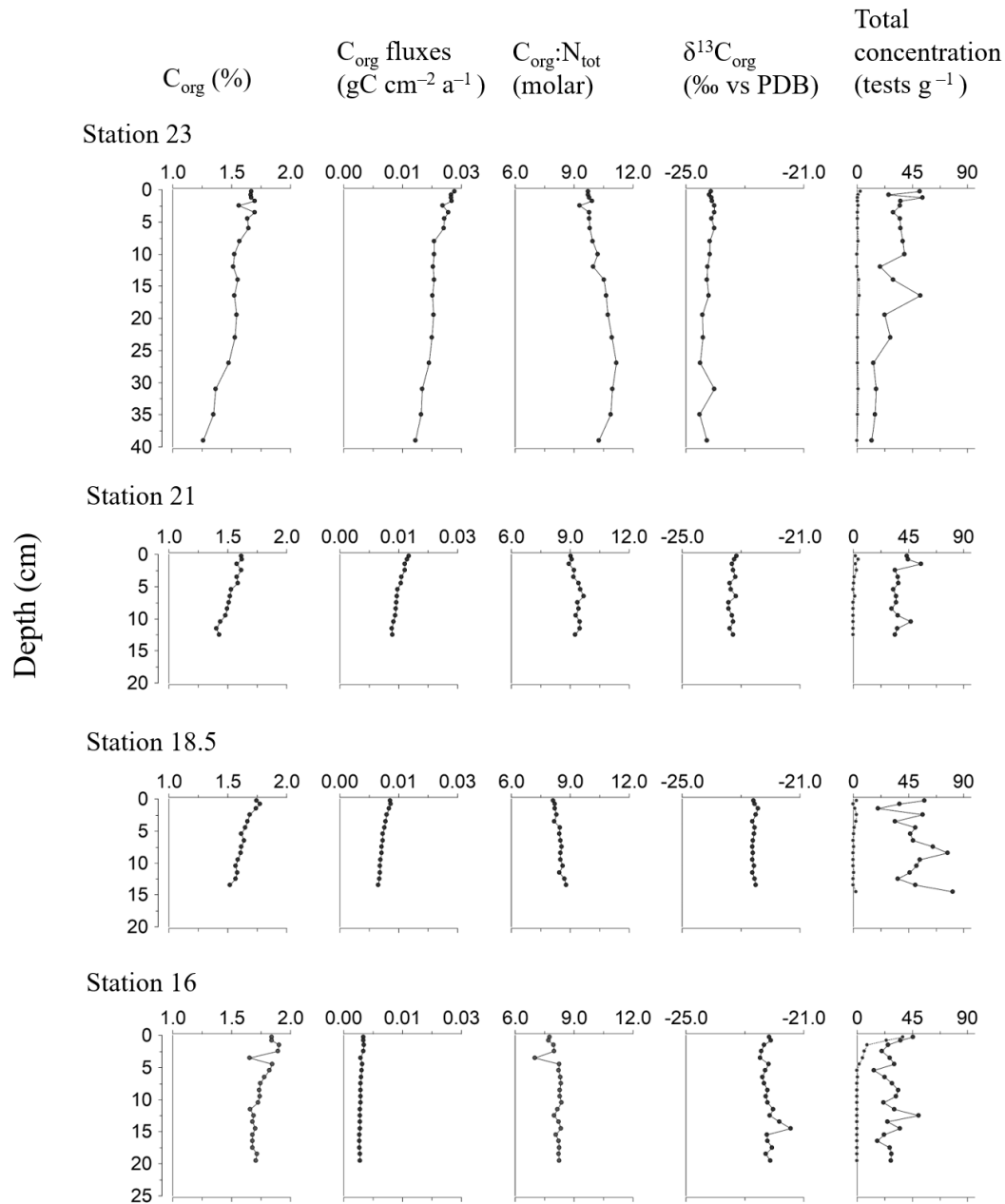
Figure 1.4   Organic carbon content (C_{org}, %w/w), organic carbon to total nitrogen molar ratio (C:N), $\delta^{13}C$ of organic carbon, total foraminiferal test concentrations (dashed lines for agglutinated), and C_{org} fluxes as a function of depth, at station 23, station 21, station 18.5 and station 16.

1.4.3   Composition and species diversity of the benthic foraminiferal assemblages

The abundance of benthic foraminifera ranges between 11 and 81 tests per g of sediment. Concentrations are higher towards the upper part of the core in the LSLE, while no clear trend is observed for cores in the GSL. Specimens of calcareous and agglutinated taxa were well preserved, with few broken or altered tests. Some slightly twisted or crooked test specimens of *Brizalina subaenariensis* and *Eubuliminella exilis* were occasionally found in all cores. A total of 52 calcareous and 4 agglutinated taxa were identified in the >63 µm fraction of the 4 study cores. Among those, 7 calcareous taxa are common to abundant at all stations, representing >10% of the assemblages in many samples: *Brizalina subaenariensis*, *Eubuliminella exilis*, *Globobulimina auriculata*, *Bulimina marginata*, *Nonionellina labradorica, Pullenia osloensis*, and *Elphidium clavatum*. Additionally, nearly 25 taxa are considered occasional, whereas 20 taxa are considered rare as they account for <3% of the assemblages in samples of each core.

A total of 26, 36, 44 and 40 calcareous species were identified, respectively, in the cores recovered from stations 23, 21, 18.5 and 16 (see Table A2). We observe a loss in the number of species towards the core top at all stations, indicating a loss of diversity over time (Fig. 1.5). In the LSLE, at station 23, the number of species decreased by about 60% since the 1960s. In the GSL, at station 16, species diversity dropped by almost 65% over the same time period, while the entire sedimentary record shows a decrease of 75% over the last ~160 years. The number of species decreases by about 50% over the last ~30 years at station 21, and by about 60% over the last ~50 years at station 18.5.

A Station 23
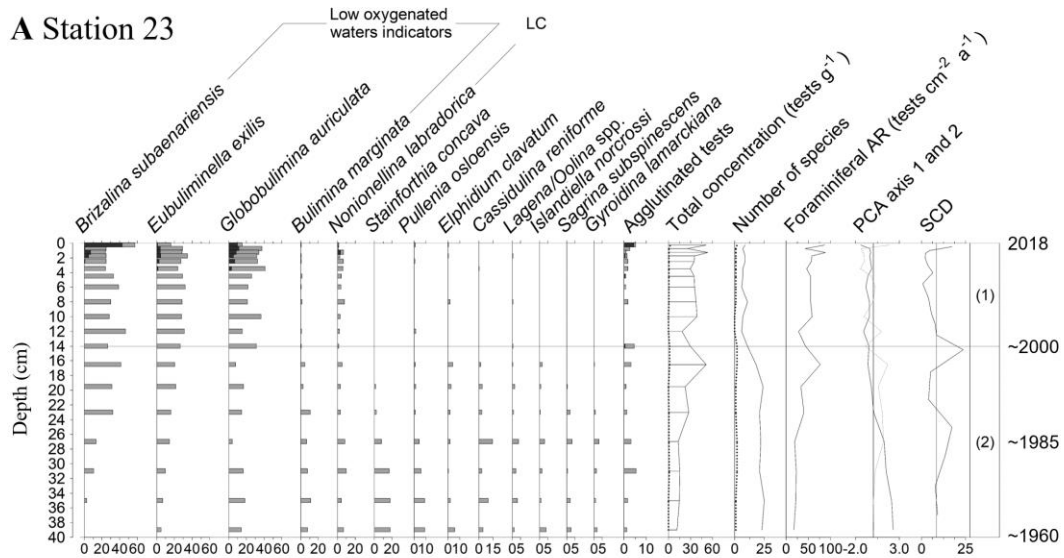
B Station 21
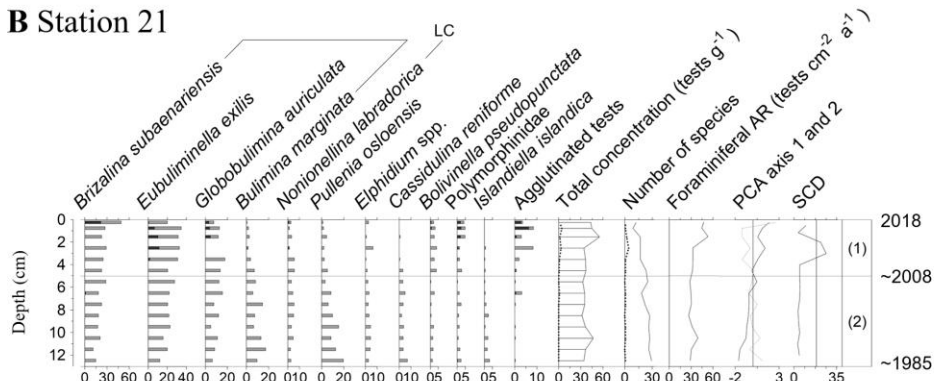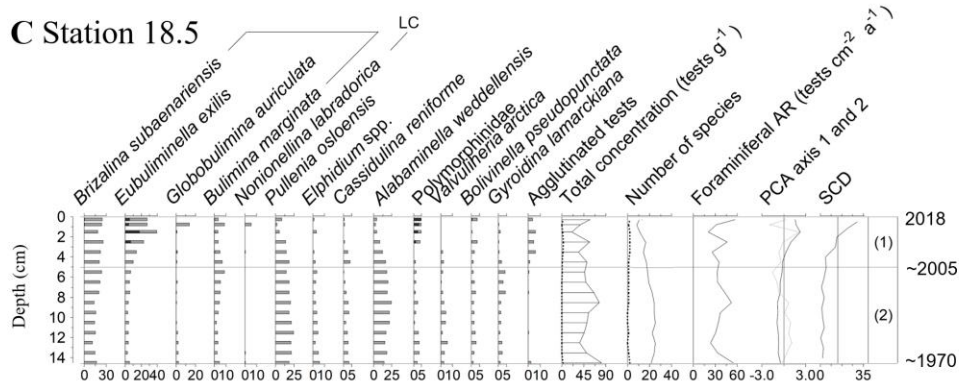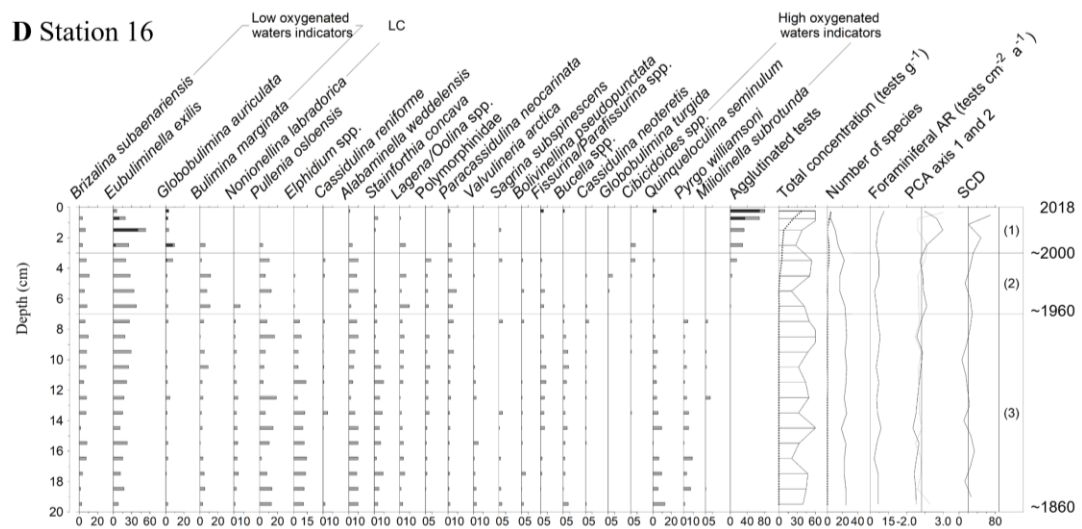
C Station 18.5

Figure 1.5   Benthic foraminiferal assemblages from A) station 23, B) station 21, C) station 18.5, and D) station 16. Relative abundance of the main taxa (≥ 3% in at least one sample), total concentration (tests g^{-1}), number of species, accumulation rates (tests cm^{-2} a^{-1}), scores of principal component analysis (PCA), and squared chord distance (SCD) coefficient, as a function of depth. The black portion of the histograms indicates the percentage of stained (living) specimens. The dotted lines in the total concentration and number of species diagrams correspond to the agglutinated tests. The PC1 score is given by the black solid line and the PC2 score is presented by the grey line. Horizontal grey lines and numbers in brackets indicate zones defined by PCA scores explained in the text.

At station 23, living specimens of *Brizalina subaenariensis*, *Eubuliminella exilis*, *Globobulimina auriculata*, *Nonionellina labradorica*, and agglutinated species are mostly found in the top 4 cm of the sediment core, which corresponds to the mixing depth (Fig. 1.3). Maximum abundances of partially tainted specimens of *B. subaenariensis, E. exilis*, and *G. auriculata* occurred, respectively at sub-bottom depths of 25 cm, 15 cm and 14 cm. Living specimens of *B. subaenariensis*, *E. exilis*, *G. auriculata*, *B. marginata*, Polymorphinidae, and agglutinated species were mostly found in the upper 6 cm of the core at station 21, and in the upper 3 cm of the core at station 18.5. Partially stained individuals, mostly of *B. marginata*, were observed throughout the cores. In the core from station 16, living specimens of *Quinqueloculina seminulum, Paracassidulina neocarinata, Buccella* spp. (mostly *B. frigida*), and agglutinated taxa were observed in the upper first cm and living specimens of *E. exilis* and *G. auriculata* were mostly observed in the upper 3 cm. Partially tainted specimens of *G. auriculata* were found down to a depth of 8 cm.

In the LSLE, the overall assemblage is dominated by the calcareous taxa *Brizalina subaenariensis*, *Eubuliminella exilis*, *Globobulimina auriculata*, *Bulimina marginata*, *Nonionellina labradorica,* and *P. osloensis* (Fig. 1.5A, B), which together account for ~84% of the assemblage in the core from station 23 and for ~79% of the assemblage in the core from station 21. The most important secondary taxa in the LSLE include *Cassidulina reniforme* and *Elphidium clavatum*. The assemblage at station 23 resembles the one described by Thibodeau et al. (2006) in the >106 μm fraction from a core taken at the same station nearly two decades earlier. A much lower species diversity was, however, reported by Thibodeau et al. (2006). The discrepancy could be due to the differential size fraction analyzed. Our analyses indicate that about 40% of species were exclusively recovered in the 63−106 μm fraction (see Table A3).

In the GSL, we observe a higher diversity than in the LSLE with assemblages dominated by *B. subaenariensis*, *E. exilis, P. osloensis*, and *Alabaminella weddellensis*

which together account for a ~67% of the assemblage at station 18.5. At station 16, they are dominated by *E. exilis* and *P. osloensis*, which account for ~40% of the assemblage. Secondary species include *C. reniforme*, *Elphidium* spp. (mostly E. *clavatum*), *G. auriculata*, *B. marginata*, and *N. labradorica*.

B. subaenariensis is the dominant species in all study cores, except at station 16 where *E. exilis* dominates. This suggests that *B. subaenariensis* has a higher tolerance for reduced oxygen levels than *E. exilis*, since the bottom-water DO concentration is currently much higher (~117 µM) at station 16 than at stations in the western part of the LC (<80 µM; Fig. 1.8).

1.4.4   Multivariate analyses

The principal component analyses (PCA) are presented in Figure 1.6. In the core from station 23, the first axis (PC1) shows an opposition between species that are less tolerant to hypoxic conditions (*Elphidium clavatum* and *Pullenia osloensis*) on the positive side and taxa that tolerate low oxygen levels (*Brizalina subaenariensis*, *Eubuliminella exilis*, and *Globobulimina auriculata*) on the negative side. The second axis (PC2) shows positive scores for *B. subaenariensis* and all secondary species, while *E. exilis* and *G. auriculata* yield negative scores (Fig. 1.6A). In the core from station 21, PC1 shows an opposition between *G. auriculata, N. labradorica, B. marginata*, *Elphidium* spp., *C. reniforme, P. osloensis*, and *Islandiella islandica* on the negative side and *B. subaenariensis*, *E. exilis*, *Bolivinella pseudopunctata*, and Polymorphinidae species on the positive side (Fig. 1.6B). Although the ecological interpretation of this analysis is not as clear as for station 23, there seems to be a similar opposition between low diversity and high diversity assemblages, potentially as a result of changes in overlying water oxygenation conditions. At station 18.5, PC1 shows an opposition between the dominant taxa (*B. subaenariensis*, *E. exilis*, *G. auriculata*, *B. marginata*), *N. labradorica* and Polymorphinidae on the positive side and all other taxa on the

negative side (Fig. 1.6C). In the core from station 16, PC1 seems to show an opposite trend between some low-oxygen tolerant species that display affinities for warm water and species characteristic of cold waters, whereas PC2 seems to oppose low-oxygen tolerant species to other taxa (Fig. 1.6D). Three main assemblage zones were defined based on these PCA results, and their boundaries were set using both PC1 and PC2, and maximum SCD coefficients (Fig. 1.5).

Zone 1 is generally characterized by the dominance of *B. subaenariensis, E. exilis, G. auriculata*, which are low-oxygen tolerant species (Kaiho, 1994; Sen Gupta, 1999; Brüchert et al., 2000), as well as by a low diversity of species. It encompasses approximately the last 20 years, from the early 2000s to 2018, as derived from the age model in the core from station 23.

Zone 2 is likely a transitional zone, as it corresponds to a decrease in species diversity and the successive decrease or disappearance of most occasional taxa, such as *B. marginata, P. osloensis, E. clavatum*, as well as an increased abundance of *B. subaenariensis, E. exilis*, and *G. auriculata*. It encompasses from about ~1960 to ~2000 in stations 23 and 16.

Zone 3 is observed in the lower part of the core from station 16. It is characterized by the highest taxonomical diversity, low percentages of *B. subaenariensis* and *G. auriculata*, and the common occurrence of *E. exilis*, *P. osloensis* and *E. clavatum*, as well as the indicator of well-oxygenated waters *Quinqueloculina seminulum* (Kaiho, 1994).

The significant loss in species diversity and the change towards assemblages dominated by low oxygen-tolerant taxa between Zone 1 and 2 around the late 1990s and early 2000s in all four cores illustrate how rapidly benthic foraminifera responded to the changes in ocean circulation happening at the same time (Jutras et al., 2020a).
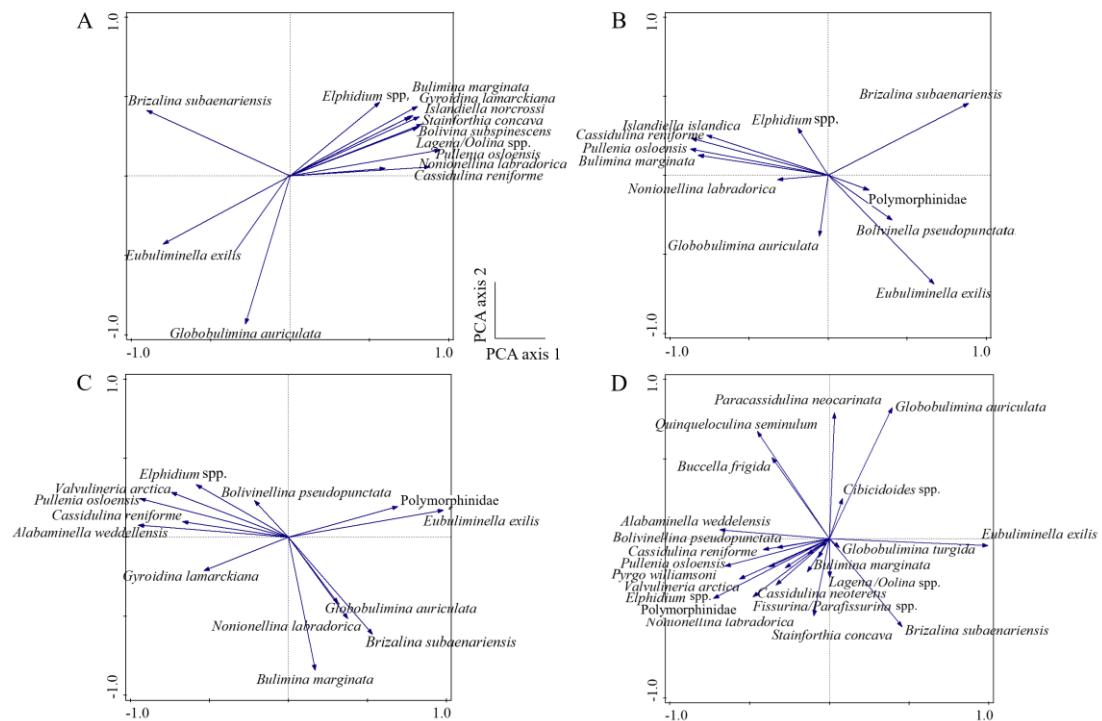
Figure 1.6   Ordination diagrams of benthic foraminiferal taxa (≥ 3% in at least one sample). A) station 23 (n = 13). PCA axes 1 and 2, respectively, explain 61% and 30% of the variance. B) Station 21 (n = 11). PCA axes 1 and 2, respectively, explain 60% and 20% of the variance. C) Station 18.5 (n =13). PCA axes 1 and 2, respectively, explain 81% and 7% of the variance. D) Station 16 (n =24). PCA axes 1 and 2, respectively explain 66% and 10% of the variance.

The data from station 23, where instrumental measurements of bottom-water conditions are available for an extended period of time (~90 years), allowed us to perform an RDA to further evaluate the relationship between bottom-water temperatures, DO concentrations, and the downcore measurements of geochemical variables with benthic foraminiferal assemblages (Fig. 1.7; Table S1). The RDA reveals that oxygenation is the principal environmental parameter affecting the calcareous benthic foraminiferal assemblages in our study area, as it is highly correlated with the RDA axis 1 ($R^2 = 0.90$), which explains 52% of the variance. The relationship with food quality, as illustrated by the $C_{org}:N_{tot}$ and $\delta^{13}C_{org}$, also stands out as an important environmental parameter, as suggested by the RDA axis 2 ($R^2 = 0.42$ and $R^2 = 0.40$ respectively), which explains 11% of the variance.
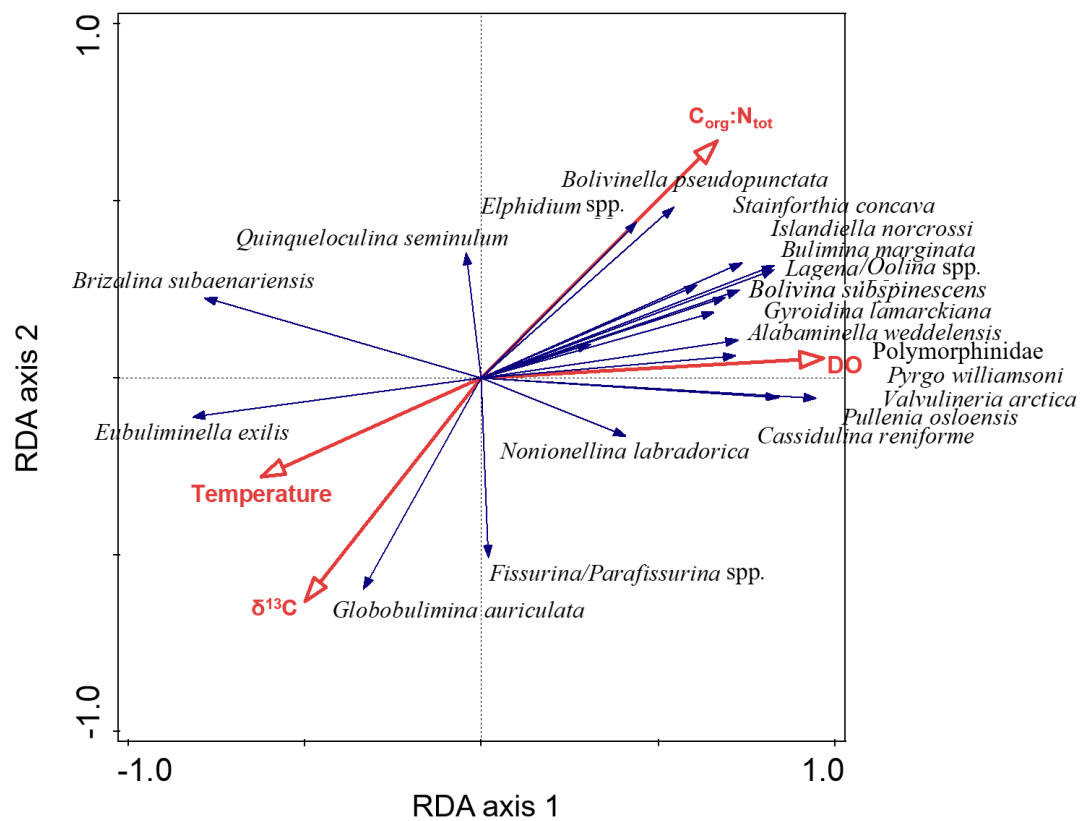
Figure 1.7   Ordination diagram of RDA of benthic foraminiferal taxa (n = 19; ≥3% of the calcareous assemblage in at least one sample), with dissolved oxygen (DO), temperature, organic carbon to total nitrogen molar ratio (C:N), and $\delta^{13}C$ of organic carbon, as environmental variables at station 23 (see Table S2). RDA axes 1 and 2, respectively, explain 52% and 11% of the variance.

1.5   Discussion

1.5.1   Mix of water masses lead to complex benthic foraminiferal assemblages

The foraminiferal assemblages of the LSLE and the GSL include a number of species that are today found in Arctic and subarctic environments (e.g., *C. reniforme*, *I. islandica, Islandiella norcrossi*, *N. labradorica*, *S. concava*, *Valvulineria arctica*; Osterman et al.,1999; Lloyd et al., 2007; Jennings et al., 2020; Cage et al., 2021; Ovsepyan et al., 2021). However, we also identified species that are today abundant in temperate to subtropical regions. Noteworthy are *Sagrina subspinescens* (commonly named *Bolivina subspinescens*), a relatively warm Atlantic Water species (Rasmussen & Thomsen, 2004), and *P. neocarinata*, a species found along the western Atlantic margin from the Gulf of Mexico to the coast of Nova Scotia (Cushman, 1922; Phleger & Parker, 1951 : all as *C. laevigata* var. *carinata*, Cushman; Parker, 1954; Vilks & Rashid, 1976: as *C. laevigata*; Sen Gupta & Aharon, 1994; Platon, 2001; Cage et al., 2021). Moreover, many of the species we observe are known to tolerate low bottom-water oxygenation (*B. subaenariensis, E. exilis*, *G. auriculata*, and *B. marginata*), including *P. neocarinata* that has also been reported to tolerate the hypoxic conditions that develop seasonally in the Gulf of Mexico (Tichenor, 2013). This complex combination of species may be explained by inputs from three different water masses into the GSL (Fig. 1.2): the LCW that brings oxygen-rich polar water, the NACW that supplies oxygen-poor warm water, and freshwater from St. Lawrence River that brings nutrients from a large watershed.

1.5.2   Benthic foraminifera and environmental conditions in the LSLE and GSL

In response to the recent changes in the ocean circulation in the northwestern Atlantic Ocean, the consequent modification of benthic environmental conditions in the GSL

(Genovesi et al., 2011; Thibodeau et al., 2018; Jutras et al., 2020a), and the development of hypoxic waters (Jutras et al., 2022), benthic foraminiferal assemblages swiftly shifted towards the quasi-exclusive dominance of low-oxygen tolerant or indicator species (i.e., *B. subaenariensis, E. exilis*, and *G. auriculata;* Figs. 1.8, 1.9) at the expense of the other taxa (Fig. 1.5). At station 23, where hypoxic conditions (<62.5 µM) have been persistent for nearly 40 years, these three taxa make up 90% of the calcareous assemblage. The overall higher species diversity at stations 18.5 and 16 is thus likely linked to the higher DO levels in the bottom waters of the GSL. Although, until 2020, hypoxic waters have only made occasional incursions into the western GSL (Jutras et al., 2022), these incursions are reflected in the important decrease of species diversity throughout the LC (Fig. 1.8).

At stations 18.5 and 16 in the GSL, the lack of long-term instrumental record of DO prevents defining quantitative relationships with foraminiferal assemblages and the relative abundances of *B. subaenariensis* and *E. exilis*. Both species are present from the base of the study cores, dating back to ~1860s at station 16, and their abundance varies little throughout the cores, especially at station 16 (Fig. 1.5D). The increase of *E. exilis* at station 16 seems to be fostered by temperature and/or higher inputs of NACW into the GSL, as this species prefers warmer waters (Caralp, 1989; Kaiho, 1994; McKay et al., 2015, 2016; Tetard et al., 2021a). The abundance of *B. marginata* and *P. neocarinata*, two other warmer-water species (Murray, 1991; Sen Gupta & Aharon, 1994; Platon, 2001), also increases towards the top of the sequence before disappearing between the late 1990s and the early 2000s at station 16, while the abundance of the colder-water species *N. labradorica*, *P. osloensis*, *E. clavatum*, and *V. arctica* (Vilks, 1969; Schafer & Cole, 1986; Knudsen et al., 1996; Polyak et al., 2002; Rytter et al., 2002) decreases (Fig. 1.5D). The increase in warmer-water species at the expense of colder-water species, paired with the disappearance of *N. labradorica,* a species associated with the LCW (Bilodeau et al., 1994), in the early 1960s in the GSL reflects changes in the relative contribution of parental waters to the LC observed

in recent decades, more specifically a lower contribution of the LCW relative to the NACW (Gilbert et al., 2005; Jutras et al., 2020a, 2022).

With the DO concentrations highlighted as the principal environmental parameter affecting benthic foraminifera, the results of the PCA in all analyzed samples (see Fig. 1.10), combined with ecological notes from the literature, have led us to define three main groups of benthic foraminifera in relation to the oxygenation conditions of their habitat.

The first group, characterized by *B. subaenariensis, E. exilis* and *G. auriculata,* is related to hypoxic bottom-water conditions ([*DO*] = <62.5 µM) in the LC. This assemblage is typically associated with Zone 1 assemblages at stations in the LSLE.

The second group is characterized by the presence of *Islandiella islandica*, *A. weddellensis*, *Gyroidina lamarckiana*, *P. osloensis*, and *Bolivinellina pseudopunctata*. It corresponds to varying, but on average relatively low bottom-water DO concentrations. Based on data from station 23, we estimate that this group corresponds to bottom-water DO concentrations ranging between 62.5 and ~100 µM.

 The third group is characterized by the presence of *Paracassidulina neocarinata*, *Buccella* spp., *Lagena/Oolina* spp., *Q. seminulum*, *Pyrgo williamsoni*, *Stainforthia concava*, and *Elphidium* spp. It would be an indicator of relatively high bottom-water oxygen levels in the LC. Data from station 23 led us to estimate that this group corresponds to bottom-water DO concentrations ranging from ~100 to ~140 µM.

It should be noted that these groups are specific to the LC, LSLE and GSL, and that their relationships with DO concentrations may not apply to the global ocean. Furthermore, the benthic environmental conditions defined by these groups are likely to have changed through time. Although bottom-water oxygenation conditions in the LSLE have been low over the past 40 years, there may have been episodic pulses of higher oxygen concentrations, as suggested by the variability of the areal extent of the

hypoxic zone (Jutras et al., 2022) and the co-occurrence of both high and low oxygen-tolerant species in groups 2 and 3.
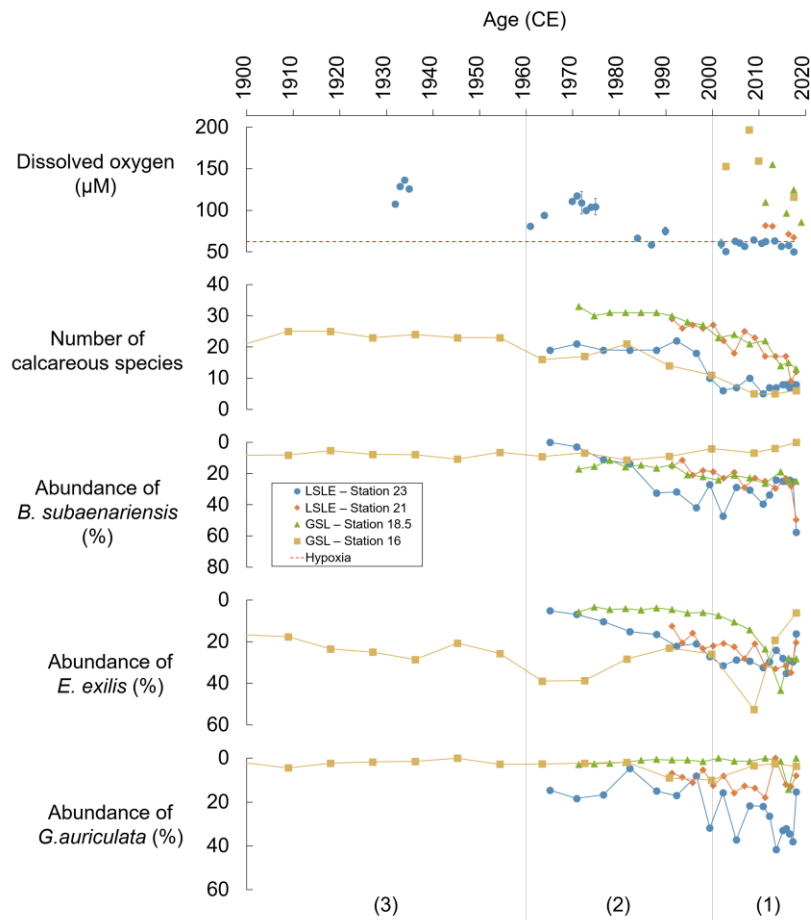
Figure 1.8   Record of dissolved oxygen concentrations at 250 to 355 m of water depth in the LSLE based on data extracted from the BioChem database made available by the Department of Fisheries and Oceans Canada, and a compilation of data acquired on the *R/V Coriolis II* (extended from Gilbert et al., 2005; Jutras et al., 2020a, see Table S1). The number of calcareous species, and percentages of *B. subaenariensis*, *E. exilis*, and *G. auriculata*. The dotted line indicates the severe hypoxia threshold (< 62.5 µM). Vertical grey lines and numbers in brackets indicate zones defined by PCA scores and correspond to the zones described in Figure 1.5.
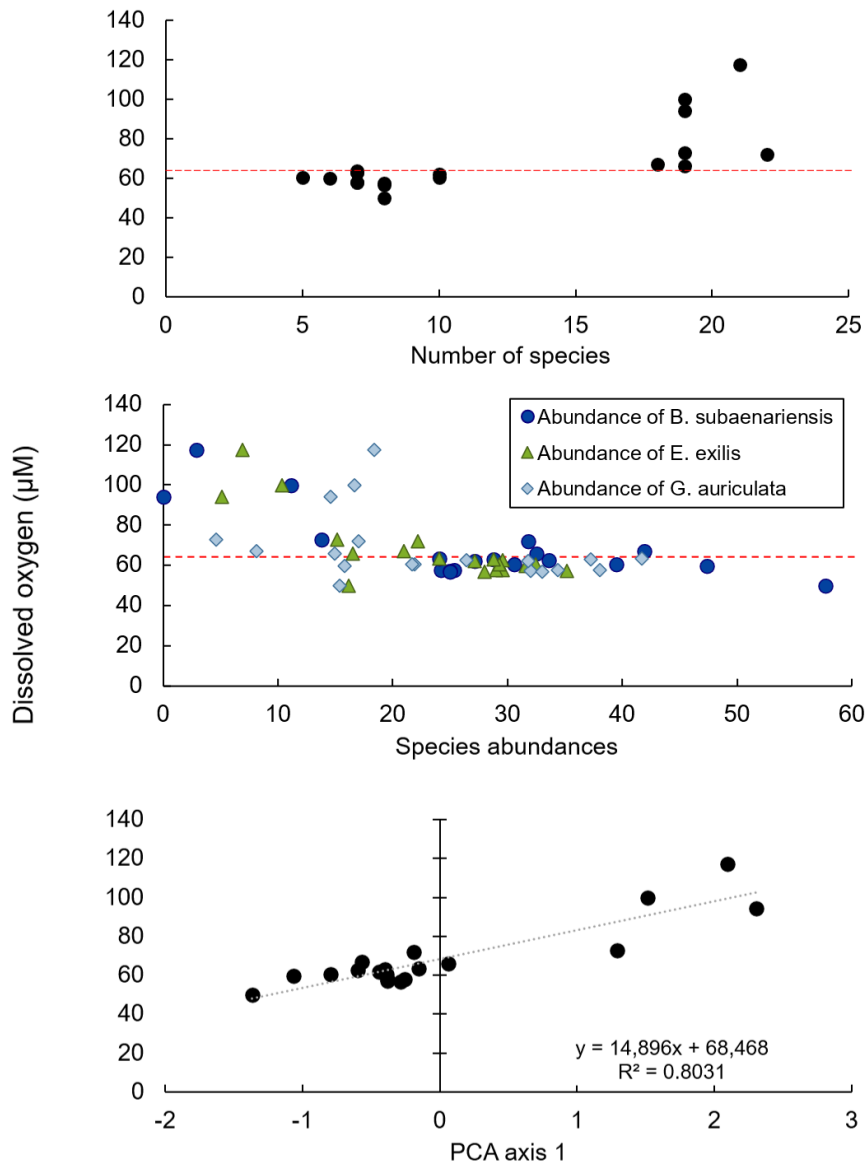
Figure 1.7   Relation between dissolved oxygen concentrations (µM), number of foraminifera species, abundance of the three most dominant taxa, and PCA axis 1 score of foraminiferal assemblages at station 23 in the LSLE. The dotted red line indicates the severe hypoxia threshold (<62.5 µM). The regression could be used as a local transfer function to reconstruct dissolved oxygen concentrations with an error (one standard deviation) of ±7.5 µM.
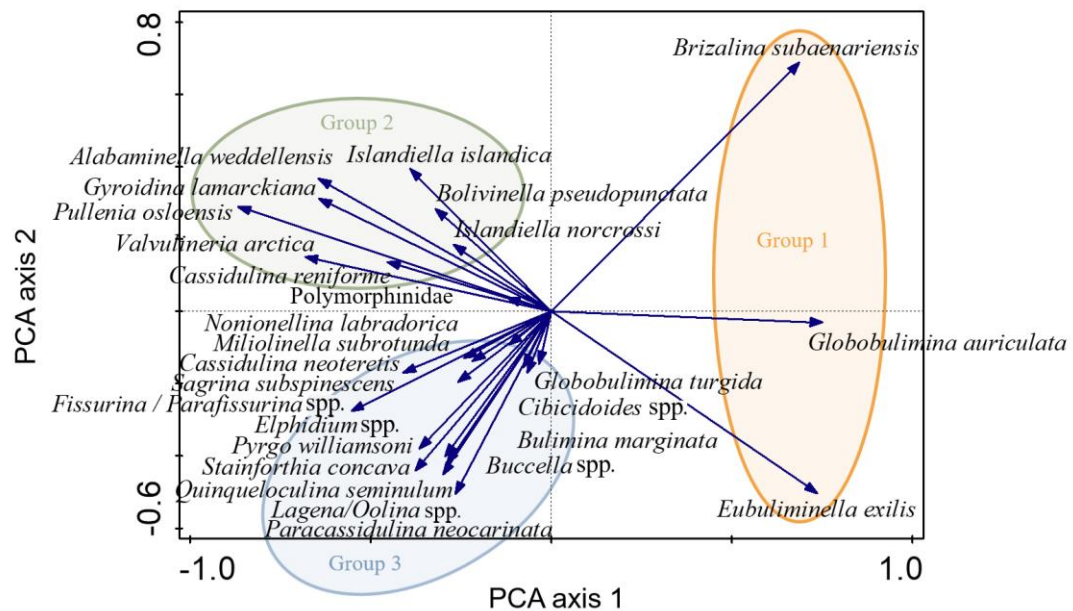
Figure 1.8   Ordination diagram of benthic foraminiferal taxa (n = 27; ≥3% in at least one sample) using the results from all stations. PCA axes 1 and 2, respectively, explain 47% and 20% of the variance. The yellow circle includes species of Assemblage 1. The blue circle includes species of Assemblage 2. The orange circle includes species of Assemblage 3.

1.5.3   Perspective on historical and longer time scales

From a recent historical perspective, the work of Hooper (1975) and Rodrigues & Hooper (1982) is interesting as it documents the distribution of benthic foraminifera in the LC in grab samples collected in the 1960s. Hence, a comparison between their data and ours (Table 1.2) allows for a further assessment of the evolution of the benthic environment for over several decades. The taxonomy of some species evolved in the last 45 years, which required some nomenclature adjustments. In Table 1.2, the original taxon names referred to by Hooper (1975) and Rodrigues & Hooper (1982) are given in brackets and we refer the reader to the appendix for taxonomical notes. Moreover, because of possible confusion in the identification of small individuals (<106 µm) at the species level, we have grouped some species of the genera *Bulimina*, *Cassidulina* and *Nonionella*. Among those, both *Bulimina marginata* and *Bulimina aculeata* are indicators of poor oxygenation and enhanced organic matter fluxes (Corliss, 1985; Jorissen et al., 1992; Mackensen et al., 1993; Sen Gupta & Machain-Castillo, 1993). Also, the species identified as *Fursenkoina loeblichi* by Rodrigues & Hooper (1982) is referred here as *Stainfothia concava* after studying specimen photographs taken by the authors.

The most notable difference between our results and those of Hooper (1975) is the absence of *B. subaenariensis* in the LSLE and the overall higher taxonomic diversity. At the time of sampling by Hooper (1975) in 1965, bottom-water DO concentrations at the western edge of the GSL were likely in excess of ~95 µM (see Fig. 1.6).

In the assemblages from the GSL that were described by Rodrigues & Hooper (1982), the dominance of *E. clavatum* and *S. concava* (as *Fursenkoina loeblichi*; Rodrigues & Hooper, 1982) is a contrasting feature from what we observe in our cores, and in the GSL in general (Genovesi et al., 2011). *E. clavatum* is an opportunistic species typically associated with low organic carbon fluxes, low salinity, and relatively cold

and well-oxygenated waters (Knudsen et al., 1996; Sen Gupta, 1999; Karlsen et al., 2000), although some studies report its occurrence in oxygen-depleted waters (e.g., Sen Gupta et al., 1996). Likewise, S*tainforthia* has been described as an opportunistic genus associated with high seasonal productivity and cold waters (Alve, 1995; Gustafsson & Nordberg, 2001; Polyak et al., 2002), and *S. concava* has been associated with Arctic waters (Lloyd et al., 2007). Thus, changes from assemblages dominated by *E. clavatum* and *S. concava* to assemblages dominated by *E. exilis*, as those we observe in zone 1 of all our study cores, could result from the change in the relative contribution of the parental waters and/or the concomitant warming of the bottom waters, both of which impact the benthic ecology, including oxygenation on the sea floor. It is difficult to disentangle these interrelated parameters. Nevertheless, our data and the RDA results imply that the DO content is ultimately the primary parameter affecting the foraminifer assemblages.

Table 1.2   A comparison of taxa identified by Hooper (1975), Rodrigues & Hooper (1982) and our study in the Laurentian Channel sediments. Large circles correspond to frequent occurrences, small circles to presence, whereas "x" indicate an absence in the sediments.

Taxa (≥ 3% in at least one sample or common in other studies)	LSLE (This study)	LSLE – Hooper (1975)	GSL (This study)	GSL – Rodrigues & Hooper (1982)
Water depth (m)	325–340	274–400	389–418	>375 m
Bottom-water dissolved oxygen concentration (µM)	56.2–58.2	~95	117	<223
Size of the studied fraction (µm)	>63	>62	>63	>75
Alabaminella weddelensis	•	x	●	x

Astrononion gallowayi	·	·	·	●
Bolivinellina pseudopunctata	·	·	·	·
Brizalina subaenariensis	●	x	●	●
Buccella spp.	·	●	·	●
Bulimina marginata [*Bulimina aculeata*]	●	●	●	●
Cassidulina neoteretis [*Cassidulina teretis*]	·	·	·	x
Cassidulina reniforme	●	x	●	·
Cibicidoides spp.	·	·	·	●
Elphidium spp.	●	●	●	●
Eubuliminella exilis	●	●	●	●
Fissurina/Parafissurina spp.	·	·	·	·
Globobulimina auriculata	●	·	●	●
Globobulimina turgida	x	x	·	x
Gyroidina lamarckiana	·	x	·	x
Islandiella helenae	·	x	·	●
Islandiella islandica	·	●	·	●
Islandiella norcrossi	·	·	·	●
Lagena/Oolina spp.	·	●	●	·
Miliolinella subrotunda	x	x	·	x
Nonionellina labradorica	●	●	●	●
Paracassidulina neocarinata [*Cassidulina carinata*]	x	x	●	·
Polymorphinidae	·	·	·	·

Pullenia spp.	●	·	●	·
Pyrgo williamsoni	·	x	●	·
Quinqueloculina seminulum	·	x	●	·
Sagrina subspinescens	·	·	·	·
Stainforthia concava [*Fursenkoina loeblichi*]	●	x	●	●
Valvulineria arctica	·	x	●	x

In order to go beyond the qualitative considerations about DO, we used our data set to develop a tool to reconstruct changes in bottom-water oxygenation. To do so, we considered the PC1 score of foraminiferal assemblages from station 23. We believe that the high coefficient of correlation between PC1 and the DO concentration $(R^2 = 0.8031$; Fig. 1.9) justifies the elaboration of the following empirical equation:

$$[DO] = 14.896 \times PC1 + 68.468$$

As for the environmental interpretation of the three main groups described in 1.5.2, it should be noted that this relationship is specific to the LC in the LSLE. It might tentatively be applied to the GSL, but not to the global ocean.

We thus tentatively applied the relationship to a long-time series from the Esquiman Channel in the eastern GSL (Fig. 1.1) in an attempt to reconstruct the low oxygen event reported to have occurred between 4,000 and 6,000 years ago by Thibodeau et al. (2013). The tentative DO reconstruction presented in Figure 1.11 highlights hypoxic levels between 4,000 and 6,000 years ago.
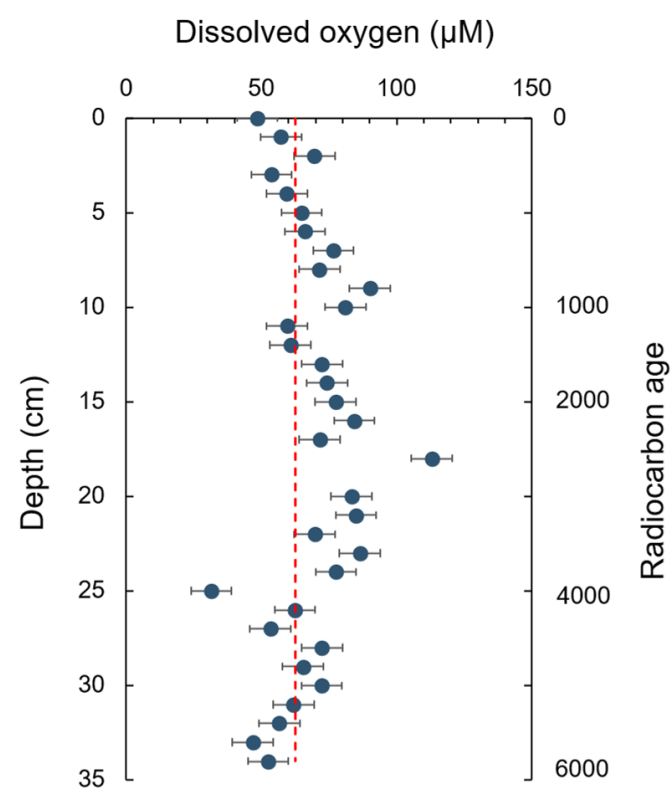
Figure 1.11   Tentative reconstruction of DO concentrations (µM) over the past 6,000 years in the Esquiman Channel applying the regression of Fig. 1.9 on the data set of Thibodeau et al. (2013; core CR06-TCE in Fig. 1.1). The dotted line corresponds to the severe hypoxia threshold (<62.5 µM), the error bar (±7.5 µM) corresponds to 1σ.

1.6   Conclusion

The micropaleontological analyses we conducted on four sediment cores from the LC documented the succession of benthic foraminiferal assemblages and their rapid spatial and temporal evolution in response to changes in benthic environmental conditions over the last few decades. The overall foraminiferal assemblages that include both cold- and warm-water species are complex. They likely relate to variations in the contribution of both oxygen-rich polar water from the LWC and oxygen-poor warm water from the NACW.

Whereas the four study sites record a decrease in taxonomic diversity of ~60–65% across the LC since the 1960s, important changes in benthic foraminiferal assemblages are observed at approximately the same time at all studied sites, around the late 1990s and the early 2000s, coincident with the areal expansion of the hypoxic zone. We observe the decrease or disappearance of most taxa in favor of hypoxia-tolerant indicator species *Brizalina subaenariensis*, *Eubuliminella exilis*, and *Globobulimina auriculata*. These changes reflect how fast benthic foraminifera assemblages respond to variations of the bottom-water DO concentrations across the LC.

Whereas other environmental parameters such as temperature could be invoked to explain multidecadal changes in the benthic microfauna, DO concentrations stand out as the major determinant parameter. Multivariate analyses highlight a close relationship between the benthic foraminiferal assemblages and bottom-water oxygen concentrations in the LSLE, from which we derived a regional proxy that allows us to estimate changes in bottom-water oxygenation prior to the period of instrumental measurements. This proxy deserves further calibration but appears promising to reconstruct the evolution of bottom-water oxygenation in relationship with large-scale changes in ocean circulation and their impact on the LSLE and the GSL during the present interglacial.

44

1.7   Acknowledgements

1.8   References

Altenbach, A. V., 1992, Short term processes and patterns in the foraminiferal response to organic flux rates: Marine Micropaleontology, v. 19, p. 119–129. doi: https://doi.org/10.1016/0377-8398(92)90024-E

Alve, E., 1995, Benthic foraminiferal distribution and recolonization of formerly anoxic environments in Drammensfjord, southern Norway: Marine Micropaleontology, v. 25, p. 169–186. doi: https://doi.org/10.1016/0377-8398(95)00007-N

Aquino-López, M.A., Blaauw, M., Christen, J.A. and Sanderson, N.K., 2018, Bayesian Analysis of [210]Pb Dating: Journal of Agricultural, Biological and Environmental Statistics, v. 23, p. 317–333. https://doi.org/10.1007/s13253-018-0328-7

Belley, R., Archambault. P., Sundby, B., Gilbert, F., and Gagnon, J.-M., 2010, Effects of hypoxia on benthic macrofauna and bioturbation in the Estuary and Gulf of St. Lawrence, Canada: Continental Shelf Research, v. 30, p.1302–1313.

Benito, X., Trobajo, R., Ibáñez, C., Cearreta, A. and Brunet, M., 2015, Benthic foraminifera as indicators of habitat change in anthropogenically impacted coastal wetlands of the Ebro Delta (NE Iberian Peninsula): Marine Pollution Bulletin, v. 101, p. 163–173. doi: https://doi.org/10.1016/j.marpolbul.2015.11.003

Benoit, P., Gratton, Y. and Mucci, A., 2006, Modeling of dissolved oxygen levels in the bottom waters of the Lower St. Lawrence Estuary: Coupling of benthic and pelagic processes: Marine Chemistry, v. 102, p.13–32.

Bernhard, J. M., 1988, Postmortem vital staining in benthic foraminifera; duration and importance in population and distributional studies: Journal of Foraminiferal Research, v. 18, p. 143–146. doi: 10.2113/gsjfr.18.2.143

Bernhard, J. M., Sen Gupta, B. K. and Borne, P. F., 1997, Benthic foraminiferal proxy to estimate dysoxic bottom-water oxygen concentrations; Santa Barbara Basin, U.S. Pacific continental margin: Journal of Foraminiferal Research, v. 27, p. 301–310. doi: 10.2113/gsjfr.27.4.301

Bernhard, J., Ostermann, D., Williams, D. and Blanks, J., 2006, Comparison of two methods to identify live benthic foraminifera: A test between Rose Bengal and CellTracker Green with implications for stable isotope paleoreconstructions: Paleoceanography, v. 21, PA4210 doi: 10.1029/2006PA001290

Bilodeau, G., de Vernal, A. and Hillaire-Marcel, C., 1994, Benthic foraminiferal assemblages in Labrador Sea sediments: relations with deep-water mass changes since deglaciation: Canadian Journal of Earth Sciences, v. 31, p. 128–138. doi: 10.1139/e94-011

Boudreau, B.P., 1986, Mathematics of tracer mixing in sediments; I, Spatially-dependent, diffusive mixing: American Journal of Science, v. 286, p.161–198. doi: https://doi.org/10.2475/ajs.286.3.199

Bourgault, D. and Koutitonsky, V. G., 1999, Real-time monitoring of the freshwater discharge at the head of the St. Lawrence Estuary: Atmosphere-Ocean, v. 37(2), p. 203–220.

Breitburg, D., 2002, Effects of hypoxia, and the balance between hypoxia and enrichment, on coastal fishes and fisheries: Estuaries, v. 25, p. 767–781. https://doi.org/10.1007/BF02804904

Brüchert, V., Pérez, M. E. and Lange, C. B., 2000, Coupled primary production, benthic foraminiferal assemblage, and sulfur diagenesis in organic-rich sediments of the Benguela upwelling system: Marine Geology, v. 163, p. 27–40. https://doi.org/10.1016/S0025-3227(99)00099-7

Bugden, G. L., 1991, Changes in the temperature-salinity characteristics of the deeper waters of the Gulf of St. Lawrence over the past several decades, *in* Therriault, J.-C., (ed.), The Gulf of St. Lawrence: small ocean or big estuary?: Canadian

special publication of fisheries and aquatic sciences, Canada, v. 113, p. 139–147.

Cage, A.G., Pieńkowski, A.J., Jennings, A., Knudsen, K.L., Seidenkrantz, M.-S., 2021, Comparative analysis of six common foraminiferal species of the genera *Cassidulina*, *Paracassidulina* and *Islandiella* from the Arctic-North Atlantic domain: Journal of Micropalaeontology, v. 40, pp. 37–60. https://doi.org/10.5194/jm-40-37-2021

Caralp, M.H., 1989, Abundance of *Bulimina exilis* and *Melonis barleeanum*: Relationship to the quality of marine organic matter: Geo-Marine Letters, v. 9, p. 37–43. https://doi.org/10.1007/BF02262816

Chabot, D. and Dutil, J. D., 1999, Reduced growth of Atlantic cod in non-lethal hypoxic conditions: Journal of Fish Biology, v. 55, p. 472–491. https://doi.org/10.1111/j.1095-8649.1999.tb00693.x

Coplen, T.B., 1995, Discontinuance of SMOW and PDB: Nature, 375(6529), p. 285. https://doi.org/10.1038/375285a0

Corliss, B. H., 1985, Microhabitats of benthic foraminifera within deep-sea sediments: Nature, v. 314(6010), p. 435–438. doi: 10.1038/314435a0

Corliss, B. H. and Emerson, S., 1990, Distribution of Rose Bengal stained deep-sea benthic foraminifera from the Nova Scotian continental margin and Gulf of Maine: Deep Sea Research Part A, Oceanographic Research Papers, v. 37, p. 381–400. doi: https://doi.org/10.1016/0198-0149(90)90015-N

Cushman, J. A., 1922, The Foraminifera of the Atlantic Ocean: United States National Museum Bulletin no. 104, pt. 3, 1–149.

D'Amours, D., 1993, The distribution of cod (*Qadus morhua*) in relation to temperature and oxygen level in the Gulf of St. Lawrence: Fisheries Oceanography, v. 2, p. 24–29. https://doi.org/10.1111/j.1365-2419.1993.tb00009.x

De, S. and Gupta, A. K., 2010, Deep-sea faunal provinces and their inferred environments in the Indian Ocean based on distribution of recent benthic foraminifera: Palaeogeography, Palaeoclimatology, Palaeoecology, v. 291, p. 429–442. doi: https://doi.org/10.1016/j.palaeo.2010.03.012

De Vernal, A., Henry, M. and Bilodeau, G., 1999, Techniques de préparation et d'analyse en micropaléontologie: Les Cahiers du GEOTOP, Montreal, 28 p.

Dickie, L. and Trites, R., 1983, The Gulf of St. Lawrence, *in* Ketchum, B., (ed.), Ecosystems of the World: Estuaries and enclosed seas: NY: Elsevier, New York, p. 403–425.

Dinauer, A. and Mucci A., 2018, Distinguishing between physical and biological controls on the spatial variability of pCO_2: a novel approach using OMP water mass analysis (St. Lawrence, Canada): Marine Chemistry, v. 204, p. 107–120. doi.org/10.1016/j.marchem.2018.03.007.

Dupont-Prinet, A., Pillet, M., Chabot, D., Hansen, T., Tremblay, R. and Audet, C., 2013, Northern shrimp (*Pandalus borealis*) oxygen consumption and metabolic enzyme activities are severely constrained by hypoxia in the Estuary and Gulf

of St. Lawrence: Journal of Experimental Marine Biology and Ecology, v. 448, p. 298–307. https://doi.org/10.1016/j.jembe.2013.07.019

Edenborn, H.M., Silverberg, N., Mucci, A. and Sundby, B., 1987, Sulfate reduction in deep coastal marine sediments: Marine Chemistry, v. 21, p. 329–345. https://doi.org/10.1016/0304-4203(87)90055-7

Eichler, P. P. B., Pimenta, F. M., Eichler, B. B. and Vital, H., 2014, Living *Bulimina marginata* in the SW Atlantic continental margin: Effect of the Subtropical Shelf Front and South Atlantic Central Water: Continental Shelf Research, v. 89, p. 88–92. doi: https://doi.org/10.1016/j.csr.2013.09.027

Erdem, Z., Schönfeld, J., Rathburn, A.E., Pérez, M.-E., Cardich, J., Glock, N., 2020, Bottom-water deoxygenation at the Peruvian margin during the last deglaciation recorded by benthic foraminifera: Biogeosciences v. 17, p. 3165–3182. doi:10.5194/bg-17-3165-2020

Fisheries and Oceans Canada (DFO), 2019, BioChem: Database of biological and chemical oceanographic data. Retrieved from http://www.dfo-mpo.gc.ca/science/data-donnees/biochem/index-eng.html

Flynn, W., 1968, The determination of low levels of polonium-210 in environmental materials: Analytica Chimica Acta, v. 43, p. 221–227.

Fontanier, C., Jorissen, F. J., Licari, L., Alexandre, A., Anschutz, P. and Carbonel, P., 2002, Live benthic foraminiferal faunas from the Bay of Biscay: faunal density, composition, and microhabitats: Deep-Sea Research I, v. 49, p. 751–785.

Galbraith, P. S., 2006, Winter water masses in the Gulf of St. Lawrence: Journal of Geophysical Research: Oceans, v. 111, p. C06022. doi: https://doi.org/10.1029/2005JC003159

Genovesi, L., de Vernal, A., Thibodeau, B., Hillaire-Marcel, C., Mucci, A. and Gilbert, D., 2011, Recent changes in bottom water oxygenation and temperature in the Gulf of St. Lawrence: Micropaleontological and geochemical evidence: Limnology and Oceanography, v. 56, p. 1319–1329.

Gilbert, D. and Pettigrew, B., 1997, Interannual variability (1948–1994) of the CIL core temperature in the Gulf of St. Lawrence: Canadian Journal of Fisheries and Aquatic Sciences, v. 54, p. 57–67.

Gilbert, D., 2004, Propagation of temperature signals along the northwest Atlantic continental shelf edge and into the Laurentian Channel, *in* Abstract, ICES CIEM annual science conference September, p. 22–25.

Gilbert, D., Sundby, B., Gobeil, C., Mucci, A. and Tremblay, G. H., 2005, A seventy-two-year record of diminishing deep-water oxygen in the St. Lawrence estuary: The northwest Atlantic connection: Limnology and Oceanography, v. 50, p. 1654–1666.

Gilbert, D., Chabot, D., Archambault, P., Rondeau, B., Hébert, S., 2007, Appauvrissement en oxygène dans les eaux profondes du Saint-Laurent marin Causes possibles et impacts écologiques. Naturaliste Canadien 131: 67-75

Gupta, A. K. and Thomas, E., 1999, Latest Miocene-Pleistocene Productivity and Deep-Sea Ventilation in the Northwestern Indian Ocean (Deep Sea Drilling Project Site 219): Paleoceanography, v. 14, p. 62–73. doi: https://doi.org/10.1029/1998PA900006

Gustafsson, M. and Nordberg, K., 2001, Living (stained) benthic foraminiferal response to primary production and hydrography in the deepest part of the Gullmar Fjord, Swedish West Coast, with comparisons to Hoglund's 1927 material: Journal of Foraminiferal Research, v. 31, p. 2–11. https://doi.org/10.2113/0310002

Hayward, B. W., Kawagata, S., Grenfell, H. R., Droxler, A. W. and Shearer, M., 2006, Mid-Pleistocene extinction of bathyal benthic foraminifera in the Caribbean Sea: Micropaleontology, v. 52, p. 245–266. doi: 10.2113/gsmicropal.52.3.245

Hoogakker, B. A. A., Lu, Z., Umling, N., Jones, L., Zhou, X., Rickaby, R. E. M., Thunell, R., Cartapanis, O., Galbraith, E., 2018, Glacial expansion of oxygen-depleted seawater in the eastern tropical Pacific: Nature v. 562, p. 410–413. doi:10.1038/s41586-018-0589-x

Hooper, K., 1975, Foraminiferal ecology and associated sediments of the lower St. Lawrence Estuary: Journal of Foraminiferal Research, v. 5, p. 218–238. doi: 10.2113/gsjfr.5.3.218

Jennings, A., Andrews, J. T., Reilly, B., Walczak, M., Jakobsson, M., Mix, A., Stoner, J., Nicholls, K.W., and Cheseby, M., 2020, Modern foraminiferal assemblages in northern Nares Strait, Petermann Fjord, and beneath Petermann Ice Tongue, NW Greenland: Arctic, Antarctic, and Alpine Research, v. 52, pp. 491–511

Jorissen, F. J., Barmawidjaja, D. M., Puskaric, S. and van der Zwaan, G. J., 1992, Vertical distribution of benthic foraminifera in the northern Adriatic Sea: The relation with the organic flux: Marine Micropaleontology, v. 19, p. 131–146. doi: https://doi.org/10.1016/0377-8398(92)90025-F

Jorissen, F. J., Fontanier, C. and Thomas, E., 2007, Paleoceanographical proxies based on deep-sea benthic foraminiferal assemblage characteristics: Developments in Marine Geology, v. 1, p. 263–325.

Jouanneau, J.M., Castaing, P., Grousset, F., Buat-Ménard, P. and Pedemay, P., 1999, Recording and chronology of a cadmium contamination by ^{137}Cs in the Gironde estuary (SW France): Comptes Rendus de l'Académie des Sciences Series IIA Earth and Planetary Science, v. 4(329), p. 265–270.

Jutras, M., Dufour, C. O., Mucci, A., Cyr, F. and Gilbert, D., 2020a, Temporal changes in the causes of the observed oxygen decline in the St. Lawrence Estuary: Journal of Geophysical Research: Oceans, v. 125, p. e2020JC016577. https://doi.org/10.1029/2020JC016577

Jutras, M., Mucci, A., Sundby, B., Gratton, Y. and Katsev, S., 2020b, Nutrient cycling in the Lower St. Lawrence Estuary: Response to environmental perturbations: Estuarine, Coastal and Shelf Science, v. 239, p. 106715. doi: https://doi.org/10.1016/j.ecss.2020.106715

Jutras, M., Mucci, A., Chaillou, G., Nesbitt, W. A., and Wallace, D. W. R., 2022, Temporal and spatial evolution of bottom-water hypoxia in the Estuary and Gulf of St. Lawrence: EGUsphere [preprint], https://doi.org/10.5194/egusphere-2022-1090

Kaiho, K., 1994, Benthic foraminiferal dissolved-oxygen index and dissolved-oxygen levels in the modern ocean, Geology, v. 22, 719–722. doi: 10.1130/0091-7613(1994)022<0719:Bfdoia>2.3.Co;2

Karlsen, A. W., Cronin, T. M., Ishman, S. E., Willard, D. A., Kerhin, R., Holmes, C. W. and Marot, M., 2000, Historical trends in Chesapeake Bay dissolved oxygen based on benthic foraminifera from sediment cores: Estuaries, v. 23, p. 488–508. doi: 10.2307/1353141

Kitazato, H., 1994, Foraminiferal microhabitats in four marine environments around Japan: Marine Micropaleontology, v. 24, p. 29–41. https://doi.org/10.1016/0377-8398(94)90009-4

Knudsen, K. L., Conradsen, K., Heier-Nielsen, S. and Seidenkrantz, M.-S., 1996. Palaeoenvironments in the Skagerrak-Kattegat basin in the eastern North Sea during the last deglaciation: Boreas, v. 25, p. 65–78. doi: https://doi.org/10.1111/j.1502-3885.1996.tb00836.x

Lloyd, J. M., Kuijpers, A., Long, A., Moros, M. and Park, L. A., 2007, Foraminiferal reconstruction of mid- to late-Holocene Ocean circulation and climate variability in Disko Bugt, West Greenland: The Holocene, v. 17, p. 1079–1091. doi: 10.1177/0959683607082548

Loeblich, A.R. and Tappan, H., 1987, Foraminiferal Genera and their Classification, Van Nostrand Reinhold 825 Company, New York, 970 p.

Loubere, P., 1994, Quantitative estimation of surface ocean productivity and bottom water oxygen concentration using benthic foraminifera: Paleoceanography, v. 9, p. 723–737. doi: https://doi.org/10.1029/94PA01624

Loubere, P. and Fariduddin, M., 1999, Benthic Foraminifera and the flux of organic carbon to the seabed, in Sen Gupta, B. K. (ed.), Modern Foraminifera: Kluwer Academic Publishers, p. 181–199. https://doi.org/10.1007/0-306-48104-9_11

Mackensen, A., Hubberten, H.-W., Bickert, T., Fischer, G. and Fütterer, D. K., 1993, The δ^{13}C in benthic foraminiferal tests of Fontbotia wuellerstorfi (Schwager) Relative to the δ^{13}C of dissolved inorganic carbon in Southern Ocean Deep Water: Implications for glacial ocean circulation models: Paleoceanography, v. 8, p. 587–610. doi: https://doi.org/10.1029/93PA01291

McKay, C. L., Groeneveld, J., Filipsson, H. L., Gallego-Torres, D., Whitehouse, M. J., Toyofuku, T. and Romero, O. E., 2015, A comparison of benthic foraminiferal Mn/Ca and sedimentary Mn/Al as proxies of relative bottom-water oxygenation in the low-latitude NE Atlantic upwelling system: Biogeosciences, v. 12, p. 5415–5428. doi: 10.5194/bg-12-5415-2015

McKay, C. L., H. L. Filipsson, O. E. Romero, J.-B. Stuut, W. and Björck, S., 2016, The interplay between the surface and bottom water environment within the

Benguela Upwelling System over the last 70 ka: Paleoceanography, v. 31, p. 266–285, doi:10.1002/2015PA002792.

Meyers, P. A., 1997, Organic geochemical proxies of paleoceanographic, paleolimnologic, and paleoclimatic processes: Organic Geochemistry, v. 27, p. 213–250. https://doi.org/10.1016/S0146-6380(97)00049-1

Moodley, L. and Hess, C., 1992, Tolerance of Infaunal Benthic Foraminifera for Low and High Oxygen Concentrations: Biological Bulletin, v. 183, p. 94–98 doi: 10.2307/1542410

Murray, J. W., 1991, Ecology and Paleoecology of Benthic Foraminifera: Longman Scientific and Technical, London, 397 p.

Murray, J. W., 2006, Ecology and applications of benthic foraminifera: Cambridge University Press, Cambridge, 426 p.

Muzuka, A. N., and Hillaire-Marcel, C., 1999, Burial rates of organic matter along the eastern Canadian margin and stable isotope constraints on its origin and diagenetic evolution: Marine Geology, v. 160, 251–270. https://doi.org/10.1016/S0025-3227(99)00022-5

Nees, S., 1997, Late Quaternary palaeoceanography of the Tasman Sea: the benthic foraminiferal view: Palaeogeography, Palaeoclimatology, Palaeoecology, v. 131, p. 365–389. doi: https://doi.org/10.1016/S0031-0182(97)00012-6

Nees, S. and Struck, U., 1999, Benthic foraminiferal response to major paleoceanographic changes, *in* Abrantes, F. and Mix, A. (eds), Reconstructing Ocean History: Springer, Boston, p. 195–216. https://doi.org/10.1007/978-1-4615-4197-4_13

Nesbitt, W. A. and Mucci, A., 2021, Direct evidence of sediment carbonate dissolution in response to bottom-water acidification in the Gulf of St. Lawrence, Canada: Canadian Journal of Earth Sciences, v. 58, p. 84–92. doi: 10.1139/cjes-2020-0020

Ohkushi, K., Kennett, J. P., Zeleski, C. M., Moffitt, S. E., Hill, T. M., Robert, C., Beaufort, L., and Behl, R. J., 2013, Quantified intermediate water oxygenation history of the NE Pacific: A new benthic foraminiferal record from Santa Barbara basin: Paleoceanography, v. 28, p. 453– 467.

Osterman, L. E., Poore, R. Z., and Foley, K. M., 1999, Distribution of benthic foraminifers (>125 μm) in the surface sediments of the Arctic Ocean: U.S. Geological Survey Bulletin, v. 2164, p. 1–28.

Osterman, L. E., 2003, Benthic foraminifers from the continental shelf and slope of the Gulf of Mexico: an indicator of shelf hypoxia: Estuarine, Coastal and Shelf Science, v. 58, p. 17–35. https://doi.org/10.1016/S0272-7714(02)00352-9

Overpeck, J.T., Webb, T.I.I.I. and Prentice, I.C., 1985, Quantitative interpretation of fossil pollen spectra: dissimilarity coefficients and the method of modern analogs: Quaternary Research, v. 23, p.87–108. doi:10.1016/0033-5894(85)90074-2

Ovsepyan, E., Ivanova, E., Tetard, M., Max, L. and Tiedemann, R., 2021, Intermediate- and deep-water oxygenation history in the subarctic North Pacific during the last deglacial period: Frontiers in Earth Science, v. 9, p. 638069.

Parker, F. L., 1954, Distribution of the foraminifera in the northwest Gulf of Mexico: Bulletin of the Museum of Comparative Zoology, v. 111, pp. 453–588.

Patterson, R.T., Guilbault, J.P. and Thomson, R.E., 2000, Oxygen level control on foraminiferal distribution in Effingham Inlet, Vancouver Island, British Columbia, Canada: Journal of Foraminiferal Research, v. 30, p. 321–335. https://doi.org/10.2113/0300321

Phleger, F. B. and Parker, F. L., 1951, Ecology of Foraminifera, Northwest Gulf of Mexico, Part II. Foraminifera Species: The Geological Society of America, Memoir, v. 46, pp. 1–64.

Platon, E., 2001, Benthic Foraminifera in Two Stressed Environments of the Northern Gulf of Mexico: LSU Historical Dissertations and Theses, v. 307, 291 p. https://digitalcommons.lsu.edu/gradschool_disstheses/307

Platon, E., Gupta, B. K. S., Rabalais, N. N. and Turner, R. E., 2005, Effect of seasonal hypoxia on the benthic foraminiferal community of the Louisiana inner continental shelf: The 20th century record: Marine Micropaleontology, v. 54, p. 263–283. https://doi.org/10.1016/j.marmicro.2004.12.004

Polyak, L., Korsun, S., Febo, L.A., Stanovoy, V., Khusid, T., Hald, M., Paulsen, B.E. and Lubinski, D.J., 2002, Benthic foraminiferal assemblages from the southern Kara Sea, a river-influenced Arctic marine environment: Journal of Foraminiferal Research, v. 32, p. 252–273. https://doi.org/10.2113/32.3.252

Rasmussen, T.L. and Thomsen, E., 2004. The role of the North Atlantic Drift in the millennial timescale glacial climate fluctuations : Palaeogeography, Palaeoclimatology, Palaeoecology, v.210, pp.101–116, https://doi.org/10.1016/j.palaeo.2004.04.005

Rodrigues, C.G.,1980, Holocene microfauna and paleoceanography of the Gulf of St. Lawrence, Ph.D. Thesis, Carleton University, 352 p.

Rodrigues, C. G. and Hooper, K., 1982, Recent benthonic foraminiferal associations from offshore environments in the Gulf of St. Lawrence: Journal of Foraminiferal Research, v. 12, 327–352. doi: 10.2113/gsjfr.12.4.327

Rytter, F., Knudsen, K. L., Seidenkrantz, M.-S., and Eiríksson, J., 2002, Modern distribution of benthic foraminifera on the North Icelandic shelf and slope: Journal of Foraminiferal Research, v. 32, p. 217–244. https://doi.org/10.2113/32.3.217

Saucier, F., Roy, F., Senneville, S., Smith, G., Lefaivre, D., Zakardjian, B., Dumais, J., 2009, Modelling of the circulation in the estuary and the Gulf of St. Lawrence in response to variations in fresh water runoff and winds: Journal of Water Science, v. 22, p. 159–176.

Schafer, C. T., and Cole, F. E., 1986, Reconnaissance survey of benthonic foraminifera from Baffin Island Fjord environments: Arctic, v. 39, p. 232–239.

Schafer, C. T., Collins, E. S. and Smith, J. N., 1991, Relationship of Foraminifera and thecamoebian distributions to sediments contaminated by pulp mill effluent: Saguenay Fiord, Quebec, Canada: Marine Micropaleontology, v. 17, p. 255–283. doi: https://doi.org/10.1016/0377-8398(91)90016-Y

Sen Gupta, B. K. and Machain-Castillo, M. L., 1993, Benthic foraminifera in oxygen-poor habitats: Marine Micropaleontology, v. 20, p. 183–201. doi: https://doi.org/10.1016/0377-8398(93)90032-S

Sen Gupta, B. K. and Aharon, P., 1994, Benthic foraminifera of bathyal hydrocarbon vents of the Gulf of Mexico: Initial report on communities and stable isotopes: Geo-Marine Letters, v. 14, p. 88–96. doi: 10.1007/BF01203719

Sen Gupta, B. K., Eugene Turner, R. and Rabalais, N. N., 1996, Seasonal oxygen depletion in continental-shelf waters of Louisiana: Historical record of benthic foraminifers: Geology, v. 24, p. 227–230. doi: 10.1130/0091-7613(1996)024<0227:Sodics>2.3.Co;2

Sen Gupta, B.K., 1999, Modern foraminifera: Kluwer Academic Publishers, Baton Rouge, 371 p.

Smart, C. W., King, S. C., Gooday, A. J., Murray, J. W. and Thomas, E., 1994, A benthic foraminiferal proxy of pulsed organic matter paleofluxes: Marine Micropaleontology, v. 23, p. 89–99. doi: https://doi.org/10.1016/0377-8398(94)90002-7

Smith, G., Saucier, F. and Straub, D., 2006, Formation and circulation of the cold intermediate layer in the Gulf of Saint Lawrence: Journal of Geophysical Research, Oceans v. 111, p. C06011.

ter Braak, C. J. and Smilauer, P., 2012, Canoco reference manual and user's guide: software for ordination, version 5.0.

Tetard, M., Beaufort, L. and Licari, L., 2017, A new optical method for automated pore analysis on benthic foraminifera: Marine Micropaleontology, v. 136, p.30–36.

Tetard, M., Ovsepyan, E. and Licari, L., 2021a, *Eubuliminella tenuata* as a new proxy for quantifying past bottom water oxygenation: Marine Micropaleontology, v. 166, p. 102016. doi: https://doi.org/10.1016/j.marmicro.2021.102016

Tetard, M., Licari, L., Ovsepyan, E., Tachikawa, K., Beaufort, L., 2021b, Toward a global calibration for quantifying past oxygenation in oxygen minimum zones using benthic Foraminifera: Biogeosciences, v. 18, p. 2827–2841. doi:10.5194/bg-18-2827-2021

Thibodeau, B., de Vernal, A. and Mucci, A., 2006, Recent eutrophication and consequent hypoxia in the bottom waters of the Lower St. Lawrence Estuary: Micropaleontological and geochemical evidence: Marine Geology, v. 231, p. 37–50.

Thibodeau, B., Lehmann, M. F., Kowarzyk, J., Mucci, A., Gélinas, Y., Gilbert, D., Maranger, R. and Alkhatib, M., 2010, Benthic nutrient fluxes along the Laurentian Channel: Impacts on the N budget of the St. Lawrence marine system: Estuarine, Coastal and Shelf Science, v. 90, p. 195–205. doi: https://doi.org/10.1016/j.ecss.2010.08.015

Thibodeau, B., de Vernal, A. and Limoges, A., 2013, Low oxygen events in the Laurentian Channel during the Holocene, Marine Geology, v. 346, p. 183–191. doi: https://doi.org/10.1016/j.margeo.2013.08.004

Thibodeau, B., Not, C., Zhu, J., Schmittner, A., Noone, D., Tabor, C., Zhang, J. and Liu, Z., 2018, Last century warming over the Canadian Atlantic shelves linked to weak Atlantic meridional overturning circulation: Geophysical Research Letters, v. 45, p. 12,376– 12,385. https://doi.org/10.1029/2018GL080083

Vilks, G., 1969, Recent Foraminifera in the Canadian Arctic: Micropaleontology, v. 15, 35–60. doi: 10.2307/1484859

Vilks, G. and Rashid, M. A., 1976, Post-glacial paleo-oceanography of Emerald Basin, Scotian Shelf: Canadian Journal of Earth Sciences, v. 13, pp. 1256–1267.

Woodroffe, S. A., 2009, Recognizing subtidal foraminiferal assemblages: implications for quantitative sea-level reconstructions using a foraminifera-based transfer function: Journal of Quaternary Science, Published for the Quaternary Research Association, v. 24, p. 215–223.

CONCLUSION GÉNÉRALE

Ce projet de maîtrise contribue à l'avancement des connaissances, puisqu'il fournit une description complète et systématique des assemblages de foraminifères benthiques récents et sub-récents dans les sédiments de l'EMSL et du GSL, ainsi qu'un portrait de leur évolution face aux changements environnementaux récents. Les travaux menés dans le cadre de la maîtrise ont livré des résultats confirmant nos hypothèses de recherche initiales sur la portée des foraminifères benthiques comme traceurs des concentrations en oxygène dissous des eaux de fond.

Les résultats d'analyses micropaléontologiques fournissent des informations originales sur la succession des espèces de foraminifères benthiques et leur évolution dans le temps et dans l'espace depuis les études de Thibodeau *et al.* (2006) et Genovesi *et al.* (2011), notamment la rapidité avec laquelle ces derniers réagissent à l'évolution spatiale de la zone hypoxique. L'approche micropaléontologique a permis de retracer de manière qualitative l'évolution des niveaux d'oxygène dissous des eaux profondes du CL au-delà de la période de mesures instrumentales ayant débuté au début des années 1930. Nous observons une diminution de la biodiversité des foraminifères benthiques au fil du temps dans les quatre stations à l'étude, ainsi qu'une évolution vers des assemblages dominées par des espèces tolérantes à l'hypoxie *Brizalina subaenariensis*, *Eubuliminella exilis* et *Globobulimina auriculata*. La relation entre les assemblages et les mesures *in situ* d'oxygène dissous de la station 23 a permis de proposer une équation empirique pour reconstituer, à une échelle locale, les variations des conditions d'oxygénation dissous dans les eaux de fond du CL dans le passé.

L'ensemble des assemblages de foraminifères, qui comprennent à la fois des espèces d'eau froide et d'eau chaude, sont complexes. Ils sont probablement liés aux variations de la contribution d'eau polaire riche en oxygène dissous du LWC et d'eau chaude pauvre en oxygène dissous du NACW.

Alors que les quatre sites d'étude enregistrent une diminution de la diversité taxonomique d'environ 60 à 65 % à travers le CL depuis les années 1960, des changements importants dans les assemblages de foraminifères benthiques sont observés à peu près au même moment à tous les sites étudiés, vers la fin des années 1990 et le début des années 2000, coïncidant avec l'expansion spatiale de la zone hypoxique. Nous observons la diminution ou la disparition de la plupart des taxons au profit des espèces tolérantes vis-à-vis l'hypoxie, soit *Brizalina subaenariensis*, *Eubuliminella exilis* et *Globobulimina auriculata*. Ces changements reflètent la rapidité avec laquelle les assemblages de foraminifères benthiques réagissent aux variations des concentrations d'oxygène dissous dans les eaux de fond à travers le CL.

Bien que d'autres paramètres environnementaux tels que la température peuvent être évoqués pour expliquer les changements multi décennaux de la microfaune benthique, les concentrations en oxygène dissous s'avèrent le paramètre déterminant majeur, tel que le révèlent les résultats des analyses multivariées. Ces analyses démontrent également une relation étroite entre les assemblages de foraminifères benthiques et les concentrations en oxygène dissous dans les eaux de fond dans le LSLE, selon laquelle nous avons dérivé un traceur régional qui nous permet d'estimer et illustrer les changements d'oxygénation des eaux de fond avant la période de mesures instrumentales.

Ce traceur requiert une calibration plus fine, mais semble prometteur pour reconstituer l'évolution de l'oxygénation des eaux de fond du CL en relation avec les changements à grande échelle de la circulation océanique et leur impact sur le LSLE et le GSL au

cours de l'interglaciaire actuel. Les travaux futurs porteront sur la calibration et l'application du proxy à des échelles spatiale et temporelle plus étendues.

Au cours des prochaines années, la prise annuelle des mesures instrumentales d'oxygène dissous dans les eaux profondes aux stations de l'EMSL et du GSL permettront de calibrer le traceur avec plus d'exactitude et de précision, en particulier pour les stations du GSL. D'autres proxy, dont la distribution d'éléments redox-sensibles, pourrait venir appuyer ce traceur.

D'un point de vue méthodologique, les différences entre les assemblages tamisés à >106 µm et à >63 µm semblent fortement justifier l'étude de la fraction >63 µm. La fraction >63 µm contenait davantage d'espèces, incluant des espèces abondantes telles que *Pullenia osloensis* et *Alabaminella weddellensis*. Il serait donc recommandé d'adopter cette méthodologie dans la perspective de travaux futurs.

ANNEXE A : PLANCHES PHOTOS

Photographies de spécimens sélectionnés de foraminifères benthiques du chenal Laurentien, prises au microscope Keyence[TM]. Toutes les barres d'échelle = 100µm.

60

Figure A1   Keyence^{TM} microscope photographs of selected benthic foraminiferal species from the Laurentian Channel. All scale bars = 100µm. **1**

Alabaminella weddellensis (Earland, 1936) **2** *Bolivina* cf. *alata* (Seguenza, 1862) **3** *Bolivinellina pseudopunctata* (Höglund, 1947) **4** *Brizalina subaenariensis* (Cushman, 1922) **5a** *Buccella frígida* (Cushman, 1922) dorsal view **5b** *B. frígida* ventral view **6** *Bulimina marginata* (d'Orbigny, 1826) **7** *Cassidulina laevigata* (d'Orbigny, 1826) **8** *Cassidulina neoteretis* (Seidenkrantz, 1995) **9** *Cassidulina reniforme* (Nørvang, 1945) **10** *Cassidulina obtusa* (Williamson, 1858) **11a** *Cibicidoides pachydermus* (Rzehak, 1886) dorsal view **11b** *C. pachydermus* ventral view **12a** *Cibicidoides wuellerstorfi* (Schwager, 1866) dorsal view **12b** *C. wuellerstorfi* ventral view **13a**, **13b** *Elphidium clavatum* (Cushman, 1930) **14** *Elphidium selseyense* (Heron-Allen & Earland, 1911) **15** *Eubuliminella exilis* (Brady, 1884) **16** *Glandulina laevigata* (d'Orbigny, 1826) **17** *Globobulimina auriculata* (Bailey, 1894)
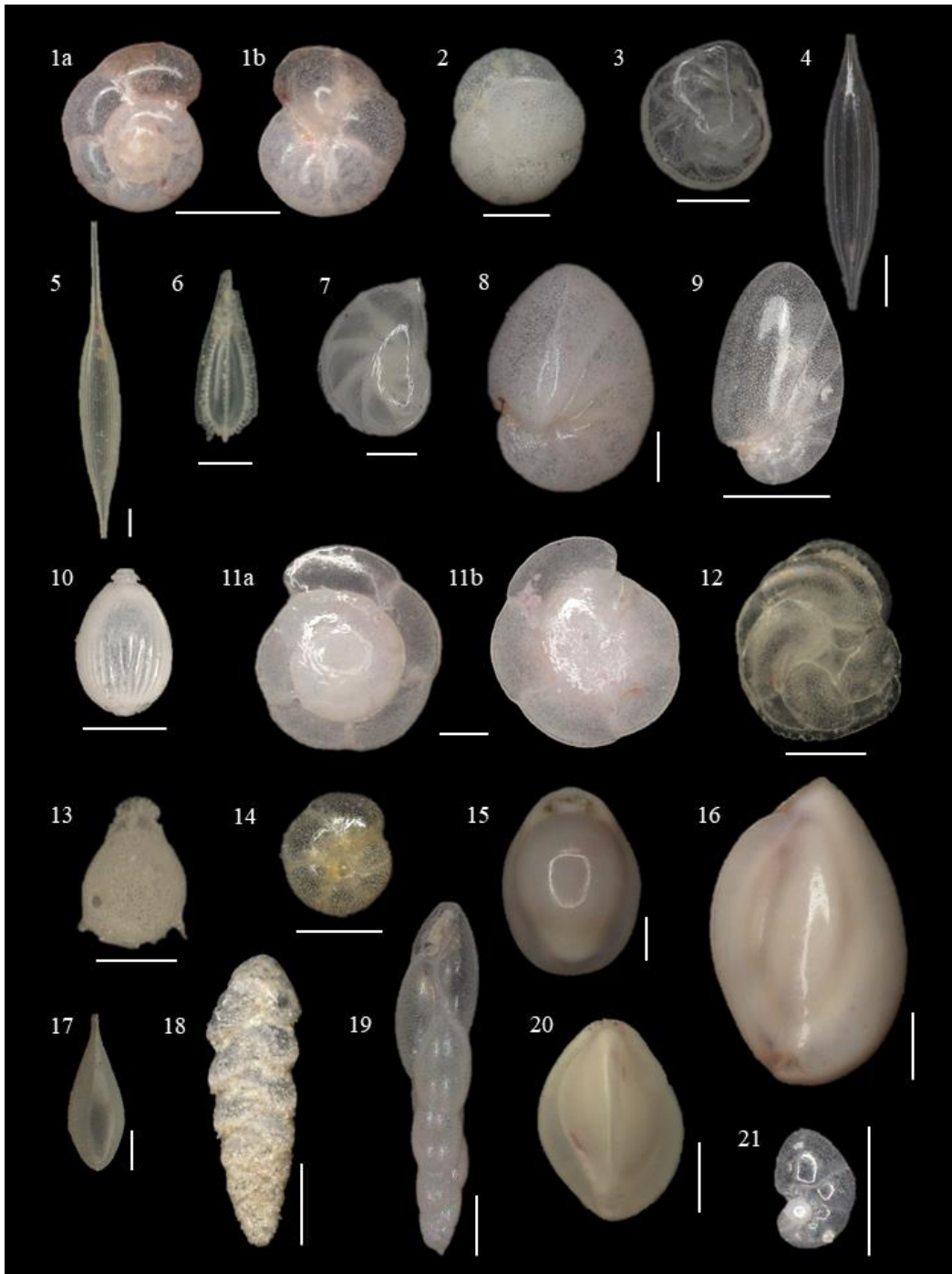
Figure A2   Keyence^{TM} microscope photographs of selected benthic foraminiferal species from the Laurentian Channel. All scale bars = 100µm. **1** *Gyroidina*

lamarckiana (d'Orbigny, 1839) **2** *Islandiella islandica* (Nørvang, 1945) **3** *Islandiella norcrossi* (Cushman, 1933) **4** *Lagena gracilis* (Williamson, 1848) **5** *Lagena mollis* (Brady, 1881) **6** *Cushmanina quadralata* (Brady, 1881) **7** *Lenticulina gibba* (d'Orbigny, 1839) **8** *Nonionellina labradorica* (Dawson, 1860) **9** *Nonionoides turgidus* (Williamson, 1858) **10** *Oolina borealis* (Loeblich & Tappan, 1954) **11a** *Oridorsalis tener* (Brady, 1884) dorsal view **11b** *O. tener* ventral view **12** *Paracassidulina neocarinata* (Thalmann, 1950) **13** *Fissurina* sp. (Reuss, 1850) **14** *Pullenia osloensis* (Feyling-Hanssen, 1954) **15** *Pyrgo williamsoni* (Silvestri, 1923) **16** *Quinqueloculina seminulum* (Linnaeus, 1758) **17** *Reussoolina laevis* (Montagu, 1803) **18** *Sagrina subspinescens* (Cushman, 1922) **19** *Stainforthia concava* (Höglund, 1947) **20** *Triloculina tricarinata* (Deshayes, 1832)* **21** *Valvulineria arctica* (Green, 1959)

ANNEXE B : LISTE ET REMARQUES TAXONOMIQUES DES
FORAMINIFÈRES BENTHIQUES DU CHENAL LAURENTIEN

Tableau A1   Liste et remarques taxonomiques pour tous les taxons de
foraminifères benthiques des sédiments du chenal Laurentien dans le LSLE et le GSL.
Les taxons sont classés par ordre alphabétique de classe et de famille.

Les taxons communs représentent >10% des assemblages. Les taxons occasionnels
constituent entre 3 et 10% des assemblages. Les taxons rares représentent <3% des
assemblages. Certains groupes taxonomiques ont été groupés dans les figures et lors
des analyses statistiques (voir *Remarks*).

Family	Genus	Species	Author	Relative abundance	Remarks
Alabaminidae	*Oridorsalis*	*tener*	Brady, 1884	Rare LSLE – GSL	
Astrononionidae	*Astrononion*	*gallowayi*	Loeblich & Tappan, 1953	Rare LSLE – GSL	
Bolivinitidae	*Bolivina*	cf. *alata.*	Seguenza, 1862	Rare LSLE – GSL	Unknown species tentatively ascribed to *B. alata*
	Bolivinellina	*pseudopunctata*	Höglund, 1947	Occasional LSLE – GSL	
	Brizalina	*subaenariensis*	Cushman, 1922	Common LSLE – GSL	
	Sagrina	*subspinescens*	Cushman, 1922	Occasional LSLE – Rare GSL	
Buliminidae	*Bulimina*	*marginata*	d'Orbigny, 1826	Common LSLE – GSL	Could have been identified as *Bulimina aculeata* in Hooper (1975) and Rodrigues & Hooper (1982)
Cancrisidae	*Valvulineria*	*arctica*	Green, 1959	Rare LSLE – Occasional GSL	
Cassidulinidae	*Cassidulina*	*laevigata*	d'Orbigny, 1826	Rare LSLE – Occasional GSL	*C. laevigata* and *C. neoteretis* are grouped in this study

		neoteretis	Seidenkrantz, 1995	Rare LSLE – Occasional GSL	
		reniforme	Nørvang, 1945	Occasional LSLE – GSL	
		obtusa	Williamson, 1858	Rare LSLE – GSL	
	Islandiella	*helenae*	Feyling-Hanssen & Buzas, 1976	Rare LSLE – Absent GSL	
		islandica	Nørvang, 1945	Occasional LSLE – Rare GSL	Referred to as *Cassidulina islandica* in Hooper (1975)
		norcrossi	Cushman, 1933	Occasional LSLE – Rare GSL	
	Paracassidulina	*neocarinata*	Thalmann, 1950	Rare LSLE – Occasional GSL	
Cibicididae	*Cibicidoides*	*pachydermus*	Rzehak, 1886	Rare LSLE – GSL	Species of the genus *Cibicidoides* are grouped in this study
		wuellerstorfi	Schwager, 1866	Rare LSLE – Occasional GSL	
		sp. A		Absent LSLE – Rare GSL	Unidentified species of *Cibicidoides*
Elphidiidae	*Elphidium*	*clavatum*	Cushman, 1930	Common LSLE – GSL	Species of the genus *Elphidium* are grouped in this study
		selseyense	Heron-Allen & Earland, 1911	Rare LSLE – GSL	
Eponididae	*Alabaminella*	*weddellensis*	Earland, 1936	Rare LSLE – Occasional GSL	
Gavelinellidae	*Gyroidina*	*lamarckiana*	d'Orbigny, 1839	Occasional LSLE – GSL	
Globobuliminidae	*Globobulimina*	*auriculata*	Bailey, 1894	Common LSLE – GSL	
		turgida	Bailey, 1851	Absent LSLE – Rare GSL	
Nonionidae	*Nonionellina*	*labradorica*	Dawson, 1860	Common LSLE – GSL	
	Nonionoides	*turgidus*	Williamson, 1858	Rare LSLE – GSL	
Pulleniidae	*Pullenia*	*osloensis*	Feyling-Hanssen, 1954	Common LSLE – GSL	
Stainforthiidae	*Stainforthia*	*concava*	Höglund, 1947	Occasional LSLE – GSL	Could have been identified as *Fursenkoina loeblichi* in Rodrigues & Hooper (1982)

		fusiformis	Williamson, 1858	Rare LSLE – GSL	
Trichohyalidae	Buccella	frigida	Cushman, 1922	Rare LSLE – Occasional GSL	
	Buccella	sp. A		Rare LSLE – GSL	Unidentified species of Buccella
Turrilinidae	Eubuliminella	exilis	Brady, 1884	Common LSLE – GSL	
Ellipsolagenidae	Cushmanina	quadralata	Brady, 1881	Absent LSLE – Rare GSL	Species of the genus Lagena, Reussoolina, Oolina and Cushmanina are grouped in this study
	Fissurina	spp.	Reuss, 1850	Rare LSLE – Occasional GSL	Fissurina/ Parafissurina, G. laevigata and Polymorphinidae are grouped together in this study
	Oolina	hexagona	Williamson, 1848	Absent LSLE – Rare GSL	Species of the genus Lagena, Reussoolina, Oolina and Cushmanina are grouped in this study
		borealis	Loeblich & Tappan, 1954		
Glandulinidae	Glandulina	laevigata	d'Orbigny, 1826	Rare LSLE – Occasional GSL	Fissurina/ Parafissurina, G. laevigata and Polymorphinidae are grouped together in this study
Hauerinidae	Parafissurina	spp.	Parr, 1947	Rare LSLE – Occasional GSL	
	Quinqueloculina	seminulum	Linnaeus, 1758	Rare LSLE – Occasional GSL	
	Triloculina	trigonula	Lamarck, 1804	Absent LSLE – Rare GSL	
		tricarinata	Deshayes, 1832	Absent LSLE – Rare GSL	
	Pyrgo	williamsoni	Silvestri, 1923	Rare LSLE – Occasional GSL	
	Miliolinella	subrotunda	Montagu, 1803	Absent LSLE – Occasional GSL	

Lagenidae					
	Lagena	*gracilis*	Williamson, 1848	Occasional LSLE – GSL	Species of the genus *Lagena, Reussoolina, Oolina* and *Cushmanina* are grouped in this study
		hispidula	Cushman, 1913		
		mollis	Brady, 1881		
		nebulosa	Cushman, 1923		
		striata	d'Orbigny, 1839		
	Reussoolina	*laevis*	Montagu, 1803		
Polymorphinidae					Various unidentified species. *Fissurina/ Parafissurina, G. laevigata* and Polymorphinidae are grouped together in this study
	Guttulina	spp.	d'Orbigny, 1839	Rare LSLE – Occasional GSL	
Spiroloculinidae					Unidentified species of *Spiroloculina*. Only a single specimen was observed
	Spiroloculina	sp. A		Absent LSLE – Rare GSL	
Vaginulinidae	*Lenticulina*	*gibba*	d'Orbigny, 1839	Rare LSLE – GSL	

ANNEXE C : DÉNOMBREMENT DES FORAMINIFÈRES BENTHIQUES

Tableau A2   Comptages bruts de tous les taxons de foraminifères benthiques. Le nombre d'individus entièrement et partiellement colorés au Rose Bengale est entre parenthèses à côté du nombre total

STATION 23

Mid-Depth (cm)	Alabaminella weddelensis	Astrononion gallowayi	Bolivinellina pseudopunctata	Brizalina subaenariensis	Bulimina marginata	Cassidulina reniforme	Elphidium clavatum	Elphidium selseyense	Eubuliminella exilis	Fissurina / Parafissurina spp.
0.25	0	0	0	75 (56)	1	1	0	0	21 (2)	2
0.75	0	0	0	18 (1)	0	0	1	0	21 (3)	1
1.25	0	0	0	45 (14)	1	0	0	0	54 (8)	5
1.5	0	0	0	32 (7)	1	1	0	0	45 (6)	1
2.5	0	0	0	25 (5)	1	0	0	0	28 (11)	1
3.5	0	0	0	26 (2)	0	0	1	0	26 (2)	0
4.5	0	0	0	42	2	0	0	0	37 (2)	1
6.5	0	0	0	45 (2)	1	0	0	0	37	0
8.5	0	0	0	48	3	3	0	0	46 (9)	0
10.5	0	0	0	44 (1)	1	0	0	0	44 (4)	0
11.5	0	0	0	36 (1)	1	0	0	0	24	0
13.5	0	0	1	35	1	0	2	0	35 (5)	0
15.5	0	2	2	88 (2)	10 (1)	9	1	0	44 (5)	1
19.5	1	3	3	112 (2)	11	11	5	1	78	1
23	2	3	6	122 (2)	41	8	6	3	62	0
27	0	0	2	21	11	3	2	1	23	1
31	0	0	1	14	10	1	5	4	13	1
35	0	3	1	5	20	4	11	2	12	0
39	2	0	3	0	11	8	13	2	7	3

Mid-Depth (cm)	Glandulina laevigata	Globobulimina auriculata	Gyroidina lamarckiana	Islandiella norcrossi	Lagena spp.	Lagena mollis	Lagena striata	Nonionellina labradorica	Oridorsalis tenerusus	Polymorphinidae
0.25	0	20 (13)	0	0	0	0	0	2 (1)	0	1
0.75	0	27 (17)	0	0	0	0	0	1	0	0
1.25	0	64 (39)	0	0	0	0	0	14 (7)	0	0
1.5	0	41 (19)	0	0	0	1	0	4	0	0
2.5	0	33 (16)	0	0	0	0	0	7 (4)	0	1
3.5	0	45 (6)	0	0	0	0	0	7 (2)	0	0
4.5	0	33	0	0	0	0	0	6	0	0
6.5	0	25	0	0	0	0	0	5	0	0
8.5	0	34 (2)	0	0	0	0	1	13 (1)	0	1
10.5	0	57	0	0	0	0	0	5 (1)	0	0
11.5	0	12 (1)	0	0	0	0	0	2	0	0
13.5	0	41 (3)	0	0	1	0	0	2	0	2
15.5	0	17	1	4	1	0	0	12	0	2
19.5	0	60 (1)	1	3	5	0	1	14	0	4
23	0	56	4	3	3	1	0	14	0	0
27	0	7	5	5	4	1	1	13	0	3
31	1	21	2	2	1	0	2	13	1	0
35	1	32	2	2	3	2	1	8	2	3
39	1	20	3	6	1	1	0	10	0	3

Mid-Depth (cm)	Pullenia osloensis	Pyrgo williamsoni	Quinqueloculina seminulum	Sagrina subspinescens	Stainforthia concava	Valvuleneria arctica	Agglutinated	Total
0.25	0	0	0	0	0	0	1	123
0.75	0	0	0	0	0	0	2	71
1.25	0	0	1	0	0	0	2	179
1.5	0	0	0	0	0	0	1	127
2.5	0	0	2	0	0	0	2	100
3.5	0	0	0	0	1	0	2	108
4.5	0	0	3	0	0	0	0	124
6.5	0	0	0	0	0	0	1	114
8.5	1	0	4	0	0	0	3	157
10.5	1	0	1	0	0	0	0	153
11.5	0	0	1	0	0	0	0	76
13.5	0	0	3 (1)	0	0	0	5	127
15.5	1	0	3	0	5	0	7	210
19.5	7	3	7	2	15	1	4	353
23	10	0	6	8	14	2	5	379
27	13	0	1	5	23	3	5	153
31	22	0	0	1	5	3	7	130
35	32	3	1	4	18	1	3	176
39	25	1	4	4	7	2	2	139

STATION 21

Mid-Depth (cm)	Alabaminella weddelensis	Astrononion gallowayii	Bolivina aff. alata	Bolivinella pseudopunctata	Brizalina subaenariensis	Bucella frigida	Bulimina marginata	Cassidulina neoteretis	Cassidulina leavigata and obtuosa	Cassidulina reniforme
0.25	0	0	0	3 (1)	68 (30)	0	1	0	0	0
0.75	0	1	0	6 (2)	52 (6)	0	4 (1)	0	0	0
1.5	0	3	2	6	52	2	6 (1)	0	0	2
2.5	0	0	1	5	35 (9)	1	2 (1)	0	0	0
3.5	0	0	0	5	46 (3)	0	7	0	1	1
4.5	0	0	2	10	57 (1)	0	18 (1)	0	1	8
5.5	0	0	1	1	71 (4)	0	21	1	1	8
6.5	0	0	0	4	29 (2)	0	9	0	1	8
7.5	0	0	0	2	54 (1)	6	35 (1)	0	0	9
8.5	1	0	3	2	49 (2)	6	20	0	1	6
9.5	0	0	1	6	48 (1)	2	18 (2)	1	3	11
10.5	3	0	1	5	62	3	39 (2)	1	3	11
11.5	0	0	3	5	29	3	44 (2)	2	1	9
12.5	1	0	2	4	43	0	27 (2)	1	2	20

Mid-Depth (cm)	Cibicidoides wuellerstorfi	Cibicidoides pseudogenerianus	Elphidium clavatum	Elphidium selseyense	Eubuliminella exilis	Fissurina/Parafissurina spp.	Glandulina laevigata	Globobulimina auriculata	Gyroidina lamarckiana	reworked (Gyroidina sp.)
0.25	0	0	1	3	28 (1)	3	0	11 (5)	0	0
0.75	0	0	0	0	65 (13)	0	0	24 (8)	0	0
1.5	0	0	0	2	71 (24)	2	0	27 (11)	0	4
2.5	3	0	4	4	39 (14)	2	0	0	0	0
3.5	0	0	0	1	58 (4)	3	0	33 (5)	0	0
4.5	0	0	2	2	52 (2)	1	1	34	0	0
5.5	0	2	2	4	69 (1)	3	0	31 (1)	0	0
6.5	0	0	4	1	34 (7)	2	1	24 (7)	0	2
7.5	0	0	4	2	49 (4)	2	2	19	0	0
8.5	1	0	3	6	57 (2)	1	2	32	0	0
9.5	0	0	5	7	62 (6)	2	2	14	1	0
10.5	0	0	6	8	47 (1)	2	0	33	0	0
11.5	0	0	6	5	52 (6)	2	2	22	0	0
12.5	0	0	3	5	35 (2)	7	2	19 (1)	0	0

Mid-Depth (cm)	Islandiella helena	Islandiella islandica	Islandiella norcrossi	Lagena hispidula	Lagena mollis	Lenticulina gibba	Nonionoides turgidus	Nonionellina labradorica	Oridorsalis tenerusus	Polymorphinidae
0.25	0	0	0	0	0	0	0	4 (2)	0	6 (3)
0.75	0	0	0	0	0	0	0	3 (1)	0	11 (5)
1.5	0	0	0	0	0	0	0	8 (2)	1	14 (5)
2.5	0	1	1	0	1	0	0	2 (1)	1	2 (1)
3.5	0	1	0	0	0	0	1	11	0	3 (1)
4.5	2	2	0	0	2	0	7	15	5	8
5.5	0	1	1	0	0	0	1	8	3	1
6.5	0	1	1	0	0	0	0	7	0	3
7.5	0	3	0	0	1	0	3	13	2	8
8.5	0	7	1	0	0	0	6	14	1	5
9.5	0	2	2	0	1	0	5	9	5	6
10.5	1	7	0	0	1	1	3	15	1	3
11.5	0	5	0	0	1	0	3	7	4	7
12.5	0	9	0	2	2	0	4	8	2	9 (1)

Mid-Depth (cm)	Pullenia osloensis	Pyrgo williamsoni	Quinqueloculina seminulum	Sagrina subspinescens	Stainforthia concava	Valvulineria arctica	Agglutinated	Total
0.25	2	0	1	0	0	0	5 (4)	136
0.75	4	0	0	0	0	0	16 (12)	186
1.5	11	0	0	0	4	0	7 (2)	224
2.5	3	0	0	0	0	0	10	117
3.5	5	0	1	0	3	0	4	184
4.5	14	1	0	0	2	1	2 (1)	249
5.5	9	0	0	0	1	2	1 (1)	243
6.5	13	0	0	0	2	0	5 (1)	151
7.5	15	1	2	0	1	1	1	235
8.5	26	2	1	0	4	3	0	260
9.5	42	1	0	0	5	2	1	264
10.5	26	0	2	0	8	1	1	294
11.5	33	1	4	1	3	1	0	255
12.5	56	0	2	0	5	6	1	277

STATION 18.5

Mid-Depth (cm)	Alabaminella weddelensis	Bolivina aff. alata	Bolivinella pseudopunctata	Brizalina spathulata	Brizalina subaenariensis	Buccella frigida	Bulimina marginata	Cassidulina leavigata	Cassidulina neoteretis	Cassidulina leavigata and obtuosa
0.25	8	0	5 (1)	0	40 (2)	4	6 (1)	0	0	0
0.75	7	0	0	0	57 (3)	0	21	0	0	0
1.5	7	0	1	0	27	0	5 (1)	0	0	0
2.5	19	1	7	0	56 (1)	0	8	0	0	0
3.5	18	2	3	0	32	0	7 (1)	0	0	0
4.5	39	1	3	0	48 (1)	0	16	0	0	0
5.5	40	0	3	0	52 (3)	1	19 (1)	0	2	0
6.5	54	0	5 (1)	0	59 (2)	0	15	1	1	0
7.5	72	0	11	0	77	2	20	0	1	0
8.5	126	2	9	1	72 (5)	3	23	0	2	0
9.5	83	2	7	0	62 (4)	0	14 (1)	3	3	2
10.5	70	7	6	0	46	3	6	2	3	0
11.5	56	2	8	0	50 (4)	0	9	1	0	1
12.5	35	0	7	1	25	0	6	4	1	1
13.5	51	2	5	0	42	2	7	5	1	0
14.5	42	0	4	0	48 (3)	1	13 (1)	0	2	1

Mid-Depth (cm)	Cassidulina reniforme	Cibicidoides wuellerstorfi	Cibicidoides pseudogerianus	Cibicidoides spp.	Cushmanina quadralata	Elphidium clavatum	Elphidium selseyense	Eubuliminella exilis	Fissurina / Parafissurina spp.	Globobulimina auriculata
0.25	1	1	0	0	0	2	0	45 (9)	0	0
0.75	2	0	0	0	0	0	0	65 (11)	1	33 (1)
1.5	0	0	0	0	0	3	2	62 (26)	1	2 (2)
2.5	2	0	1	0	0	1	0	50 (15)	1	0
3.5	4	0	3	0	0	1	1	20 (4)	0	2 (1)
4.5	10	0	1	2	0	4	1	24	2	3
5.5	1	0	2	0	0	6	2	16 (1)	1	0
6.5	3	0	0	0	0	6	1	16 (1)	2	4
7.5	7	0	1	1	0	6	2	23	4	3
8.5	16	0	2	2	0	8	5	23 (2)	2	4
9.5	13	0	3	0	2	11	3	14	4	2
10.5	5	1	6	0	1	10	3	15	1	3
11.5	8	0	2	2	0	11	4	13	4	6
12.5	7	2	2	0	0	4	1	10	4	5
13.5	8	0	2	0	0	9	5	9	4	7
14.5	10	0	1	2	0	13	4	16	2	8

Mid-Depth (cm)	Gyroidina lamarckiana	Islandiella islandica	Islandiella norcrossi	Lagena gracilima	Lagena hispidula	Lagena mollis	Lagena nebulosa	Lenticulna gibba	Miliolinella subrotunda	Nonionellina labradorica
0.25	0	0	0	0	0	0	0	0	0	0
0.75	1	0	0	0	0	0	0	0	0	13
1.5	2	0	1	0	0	0	0	0	0	0
2.5	1	0	1	0	0	1	0	0	0	2
3.5	1	0	0	0	0	1	0	0	0	1
4.5	5	2	0	0	1	0	0	1	0	0
5.5	9	2	2	0	0	0	0	1	0	0
6.5	8	7	3	0	0	1	0	1	0	3
7.5	17	5	3	2	0	0	0	1	0	1
8.5	8	12	7	0	0	1	0	2	0	1
9.5	6	10	1	0	0	0	0	2	1	2
10.5	5	3	1	0	0	0	0	0	2	1
11.5	4	3	1	0	0	2	0	0	0	1
12.5	5	3	2	0	0	0	1	0	0	2
13.5	7	2	2	0	0	0	0	0	2	5
14.5	4	4	2	1	0	0	0	0	0	2

Mid-Depth (cm)	Nonionoides turgidus	Oolina margaritae	Oridorsalis tenerusus	Paracassidulina neocarinata	Polymorphinidae	Pullenia osloensis	Pyrgo williamsoni	Quinqueloculina seminulum	Sagrina subspinescens	Stainforthia concava
0.25	0	0	0	0	23 (10)	14	0	0	1 (1)	1
0.75	0	2	0	0	18 (8)	6	0	1	1	4
1.5	0	0	0	0	10 (4)	8	0	0	0	2
2.5	1	0	2	0	9 (3)	30	0	1	1	6
3.5	0	0	1	2	0	21	0	0	1	2
4.5	0	0	2	2	3	43	0	0	1	2
5.5	0	0	2	3	4	32	0	1	0	5
6.5	2	0	2	1	4	50	0	1	3	6
7.5	2	0	2	6	4	70	0	3	3	7
8.5	4	0	5	5	14	105	0	6	4	12
9.5	0	0	10	5	6	71	0	5	1	4
10.5	1	0	7	6	2	69	0	5	3	3
11.5	2	0	6	2	10	79	0	4	5	9
12.5	0	0	6	3	8	47	1	2	1	2
13.5	4	0	1	1	10	60	1	1	2	2
14.5	1	0	5	4	7	52	1	5	1	4

Mid-Depth (cm)	Stainforthia fusiformis	Triloculina trigonula	Triloculina trihedra	Valvulineria arctica	Agglutinated	Total
0.25	0	0	0	0	6	157
0.75	0	0	0	0	1 (1)	233
1.5	1	0	0	0	9	143
2.5	0	0	0	0	10	211
3.5	1	0	0	3	9	133
4.5	0	0	0	6	4	220
5.5	0	0	0	4	2	207
6.5	0	0	0	2	1	260
7.5	0	0	0	7	2	358
8.5	0	0	0	15	1	487
9.5	0	0	0	18	0	352
10.5	0	1	0	14	0	296
11.5	0	1	0	5	2	307
12.5	0	2	0	13	0	198
13.5	0	0	0	9	1	260
14.5	0	1	2	8	7	267

STATION 16

Mid-Depth (cm)	Alabaminella weddelensis	Astrononion gallowayi	Bolivinellina pseudopunctata	Brizalina subaenariensis	Buccella frigida	Bulimina marginata	Cassidulina neoteretis	Cassidulina leavigata and obtuosa	Cassidulina reniforme	Cibicidoides spp.
0.25	1	0	0	0	1 (1)	0	0	0	0	0
0.75	0	0	0	3	0	0	0	0	0	0
1.5	0	0	0	4	0	0	0	0	0	0
2.5	2	0	0	2	0	3	0	0	0	2
3.5	11	0	1	7	0	2	0	0	2	3
4.5	9	0	0	12	0	13	1	0	2	1
5.5	13	0	2	6	0	8	0	0	0	0
6.5	2	0	0	7	1	9	1	0	0	0
7.5	9	0	2	7	1	5	3	1	2	1
8.5	22	0	0	13	3	1	1	0	1	1
9.5	9	1	0	11	5	7	1	0	1	1
10.5	6	0	0	9	5	11	1	1	1	0
11.5	6	0	1	7	4	4	1	0	2	0
12.5	3	0	1	11	2	5	1	0	1	0
13.5	7	0	1	8	2	2	0	0	5	1
14.5	27	0	1	4	6	5	1	0	1	0
15.5	13	0	1	10	2	1	1	0	0	0
16.5	9	0	0	6	1	3	0	0	0	0
17.5	14	1	5	7	3	8	0	0	0	0
18.5	24	0	1	3	1	10	0	0	0	0
19.5	17	1	2	4	5	4	1	0	3	0

Mid-Depth (cm)	Elphidium clavatum	Elphidium selseyense	Eubuliminella exilis	Fissurina / Parafissurina spp.	Glandulina laevigata	Globobulimina auriculata	Globobulimina turgida	Lagena gracilima	Lagena mollis	Lagena nebulosa
0.25	0	0	5 (1)	0	0	3 (3)	0	0	0	0
0.75	0	0	15 (8)	0	0	2 (2)	0	0	1	0
1.5	0	0	31 (24)	0	0	0	2	0	0	0
2.5	0	0	13 (2)	0	0	5 (4)	0	0	2	1
3.5	0	0	18	1	1	7 (1)	0	0	0	0
4.5	1	1	30	1	1	2	4	1	4	0
5.5	1	0	34	3	2	2	1	1	0	0
6.5	1	0	30	2	2	2 (1)	0	0	7	0
7.5	6	1	28	0	0	3 (1)	0	0	3	0
8.5	9	2	25	3	3	0	0	0	2	0
9.5	4	3	40	1	1	2	0	0	3	0
10.5	3	3	29	5	4	2	0	0	3	0
11.5	14	5	31	6	3	3	0	0	4	0
12.5	3	3	24	4	1	6	0	0	1	0
13.5	11	2	16	3	2	2	0	0	0	0
14.5	17	2	20	6	1	2	0	0	3	0
15.5	11	3	27	0	0	3	0	0	5	0
16.5	8	3	12	1	1	2	0	1	1	0
17.5	18	4	20	2	2	2	0	1	5	0
18.5	17	3	31	1	1	0	0	0	3	0
19.5	13	1	11	0	0	3	0	0	2	0

Mid-Depth (cm)	Lenticulina gibba	Miliolinella subrotunda	Nonionellina labradorica	Nonionoides turgidus	Oolina hexagona	Oridorsalis tenerusus	Paracassidulina neocarinata	Polymorphinidae	Pullenia osloensis	Pyrgo williamsoni
0.25	0	0	0	0	0	0	2 (2)	0	0	0
0.75	0	0	0	0	0	0	0	0	0	0
1.5	0	0	0	0	0	0	0	0	0	0
2.5	0	0	0	0	0	0	2	0	2	0
3.5	0	0	0	0	0	0	4	3	10	0
4.5	0	0	0	0	0	1	4	1	7	0
5.5	0	0	0	0	0	0	9	0	13	0
6.5	0	0	5	0	1	0	4	0	1	0
7.5	0	2	2	0	0	1	6	0	9	5
8.5	2	0	2	0	2	0	3	1	22	2
9.5	2	1	4	0	0	1	8	1	9	2
10.5	0	1	2	1	0	0	3	0	6	4
11.5	0	0	4	0	0	1	3	0	6	2
12.5	0	5	6	1	0	1	4	2	25	5
13.5	0	0	3	0	0	2	2	1	7	6
14.5	0	0	7	1	1	0	4	1	27	10
15.5	0	0	5	0	0	1	2	1	13	1
16.5	1	0	3	1	1	1	1	0	2	7
17.5	0	0	8	0	0	2	3	0	14	6
18.5	1	1	5	1	0	2	2	0	24	13
19.5	0	0	2	1	0	1	3	0	17	2

Mid-Depth (cm)	Quinqueloculina seminulum	Reussoolina laevis	Sagrina subspinescens	Spiroloculina sp. A	Stainforthia concava	Triloculina trigonula	Valvulineria arctica	Agglutinated	Total
0.25	3 (3)	0	0	0	0	0	0	66 (56)	81
0.75	0	0	0	0	3	0	0	52 (27)	76
1.5	0	0	1	0	1	0	0	19	58
2.5	0	0	0	0	0	0	1	15	50
3.5	2	0	2	0	0	0	0	14	88
4.5	2	2	0	0	0	1	1	6	108
5.5	0	1	0	0	2	1	0	0	99
6.5	1	0	0	0	2	0	0	1	79
7.5	1	0	3	0	3	1	0	0	105
8.5	3	2	0	0	2	1	1	0	129
9.5	7	2	0	0	6	0	0	0	133
10.5	4	2	0	0	8	0	2	0	116
11.5	6	1	0	0	17	2	3	1	137
12.5	6	0	0	0	8	0	4	0	133
13.5	6	2	3	0	9	0	0	0	103
14.5	17	1	1	0	10	0	0	0	176
15.5	1	0	0	0	8	0	6	0	115
16.5	5	0	1	1	2	0	1	0	75
17.5	16	3	0	0	16	0	3	0	163
18.5	10	0	3	0	9	0	5	0	171
19.5	17	2	3	0	5	2	4	0	126

74

Tableau A3   Comptages bruts des individus de taille entre 63 et 106µm

STATION 23

Mid-Depth (cm)	Alabaminella weddelensis	Astrononion gallowayi	Bolivinellina pseudopunctata	Brizalina subaenariensis	Bulimina marginata	Cassidulina reniforme	Elphidium clavatum	Elphidium selseyense	Eubuliminella exilis	Fissurina / Parafissurina spp.
0.25	0	0	0	1	0	1	0	0	0	2
0.75	0	0	0	2	0	0	1	0	0	1
1.25	0	0	0	1	0	0	0	0	0	5
1.5	0	0	0	3	0	1	0	0	1	1
2.5	0	0	0	1	0	0	0	0	0	1
3.5	0	0	0	1	0	0	0	1	0	0
4.5	0	0	0	1	0	0	0	0	0	1
6.5	0	0	0	2	0	0	0	0	2	0
8.5	0	0	0	2	0	3	0	0	0	0
10.5	0	0	0	1	0	0	0	0	0	0
11.5	0	0	0	3	0	0	0	0	0	0
13.5	0	0	1	0	0	0	0	0	1	0
15.5	0	0	2	12	3	9	0	0	4	1
19.5	1	0	3	9	2	10	2	1	9	1
23	2	0	6	20	8	6	3	3	10	0
27	0	0	2	7	5	3	0	0	8	1
31	0	0	1	2	3	1	1	4	2	1
35	0	0	1	1	1	1	6	0	1	0
39	2	0	3	0	5	7	9	0	3	3

Mid-Depth (cm)	Glandulina laevigata	Globobulimina auriculata	Gyroidina lamarckiana	Islandiella norcrossi	Lagena spp.	Lagena mollis	Lagena striata	Nonionellina labradorica	Oridorsalis tenerusus	Polymorphinidae
0.25	0	0	0	0	0	0	0	0	0	1
0.75	0	0	0	0	0	0	0	0	0	0
1.25	0	0	0	0	0	0	0	3	0	0
1.5	0	0	0	0	0	0	0	0	0	0
2.5	0	0	0	0	0	0	0	0	0	1
3.5	0	0	0	0	0	0	0	1	0	0
4.5	0	0	0	0	0	0	0	0	0	0
6.5	0	0	0	0	0	0	0	0	0	0
8.5	0	0	0	0	0	0	0	1	0	1
10.5	0	0	0	0	0	0	0	0	0	0
11.5	0	0	0	0	0	0	0	1	0	0
13.5	0	0	0	0	1	0	0	1	0	2
15.5	0	1	0	4	1	0	0	4	0	2
19.5	0	0	0	2	3	1	1	2	0	4
23	0	0	0	1	3	0	0	5	0	0
27	0	0	0	4	2	1	1	10	0	3
31	0	0	0	2	1	0	0	9	0	0
35	0	0	0	0	2	1	0	7	0	3
39	0	0	0	5	1	0	0	4	0	3

Mid-Depth (cm)	Pullenia osloensis	Pyrgo williamsoni	Quinqueloculina seminulum	Sagrina subspinescens	Stainforthia concava	Valvuleneria arctica	Agglutinated	Total 63 – 106 µm
0.25	0	0	0	0	0	0	0	5
0.75	0	0	0	0	0	0	0	4
1.25	0	0	0	0	0	0	0	9
1.5	0	0	0	0	0	0	0	6
2.5	0	0	0	0	0	0	0	3
3.5	0	0	0	0	0	0	0	3
4.5	0	0	0	0	0	0	0	2
6.5	0	0	0	0	0	0	0	4
8.5	0	0	0	0	0	0	0	7
10.5	0	0	0	0	0	0	0	1
11.5	0	0	0	0	0	0	0	4
13.5	0	0	0	0	0	0	0	6
15.5	0	0	0	0	3	0	0	46
19.5	0	3	0	2	6	1	0	63
23	0	0	0	8	6	2	0	83
27	0	0	0	5	15	3	0	70
31	0	0	0	1	3	3	0	34
35	0	3	0	4	13	1	0	45
39	0	1	0	4	7	2	0	59

STATION 21

Mid-Depth (cm)	Alabaminella weddelensis	Astrononion gallowayii	Bolivina aff. alata	Bolivinella pseudopunctata	Brizalina subaenariensis	Bucella frigida	Bulimina marginata	Cassidulina neoteretis	Cassidulina leavigata and obtuosa	Cassidulina reniforme
0.25	0	0	0	3	13	0	0	0	0	0
0.75	0	0	0	6	11	0	0	0	0	0
1.5	0	0	2	6	18	2	3	0	0	2
2.5	0	0	1	5	10	1	1	0	0	0
3.5	0	0	0	5	7	0	0	0	1	1
4.5	0	0	2	10	18	0	2	0	1	8
5.5	0	0	1	1	18	0	2	1	1	8
6.5	0	0	0	4	16	0	4	0	1	7
7.5	0	0	0	2	19	5	6	0	0	9
8.5	1	0	3	2	18	6	2	0	1	6
9.5	0	0	1	6	17	2	7	1	3	9
10.5	3	0	1	5	19	3	2	1	3	11
11.5	0	0	3	5	13	3	7	2	1	9
12.5	1	0	2	4	6	0	15	1	2	16

Mid-Depth (cm)	Cibicidoides wuellerstorfi	Cibicidoides pseudogenerianus	Elphidium clavatum	Elphidium selseyense	Eubuliminella exilis	Fissurina/Parafissurina spp.	Glandulina laevigata	Globobulimina auriculata	Gyroidina lamarckiana	reworked (Gyroidina sp.)
0.25	0	0	0	3	5	3	0	0	0	0
0.75	0	0	0	0	13	0	0	0	0	0
1.5	0	0	0	2	16	2	0	0	0	0
2.5	0	0	0	4	15	2	0	0	1	0
3.5	0	0	0	1	10	3	0	0	0	0
4.5	0	0	0	2	22	1	1	0	0	0
5.5	0	0	1	4	16	3	0	0	1	0
6.5	0	0	0	1	12	2	1	0	0	0
7.5	0	0	0	2	14	2	1	0	0	0
8.5	0	0	0	6	19	1	1	0	0	0
9.5	0	0	0	7	25	2	1	0	3	0
10.5	0	0	1	8	13	2	0	0	0	0
11.5	0	0	1	5	14	2	2	0	0	0
12.5	0	0	0	5	10	7	2	0	3	0

Mid-Depth (cm)	Islandiella helena	Islandiella islandica	Islandiella norcrossi	Lagena hispidula	Lagena mollis	Lenticulina gibba	Nonionoides turgidus	Nonionellina labradorica	Oridorsalis tenerusus	Polymorphinidae
0.25	0	0	0	0	0	0	0	0	0	6
0.75	0	0	0	0	0	0	0	0	0	11
1.5	0	0	0	0	0	0	0	5	1	14
2.5	0	1	0	0	0	0	0	1	1	2
3.5	0	1	0	0	0	0	1	3	0	4
4.5	0	2	0	0	0	0	5	6	3	8
5.5	0	1	0	0	0	0	1	6	3	1
6.5	0	1	0	0	0	0	0	3	0	3
7.5	0	2	0	0	0	0	3	5	2	8
8.5	0	7	0	0	0	0	6	7	1	5
9.5	0	2	0	0	0	0	5	4	5	6
10.5	0	6	0	0	0	1	3	6	1	3
11.5	0	4	0	0	0	0	3	5	3	7
12.5	0	7	0	1	2	0	4	5	2	9

Mid-Depth (cm)	Pullenia osloensis	Pyrgo williamsoni	Quinqueloculina seminulum	Sagrina subspinescens	Stainforthia concava	Valvulineria arctica	Agglutinated	Total 63 – 106 µm
0.25	2	0	0	0	0	0	0	35
0.75	4	0	0	0	0	0	0	45
1.5	11	0	0	0	2	0	0	86
2.5	3	0	0	0	0	0	0	48
3.5	5	0	0	0	2	0	0	44
4.5	14	0	0	0	1	1	0	107
5.5	9	0	0	0	0	2	0	80
6.5	13	0	0	0	1	0	0	69
7.5	15	0	0	0	1	1	0	97
8.5	26	0	0	0	2	3	0	123
9.5	42	0	0	0	2	2	0	152
10.5	26	0	0	0	3	1	0	122
11.5	33	0	0	0	0	1	0	123
12.5	56	0	0	0	1	6	0	167

STATION 18.5

Mid-Depth (cm)	Alabaminella weddelensis	Bolivina aff. alata	Bolivinella pseudopunctata	Brizalina spathulata	Brizalina subaenariensis	Buccella frigida	Bulimina marginata	Cassidulina leavigata	Cassidulina neoteretis	Cassidulina leavigata and obtuosa
0.25	8	0	6	0	15	4	1	0	0	0
0.75	7	0	0	0	6	0	0	0	0	0
1.5	7	0	1	0	14	0	2	0	0	0
2.5	19	1	8	0	39	0	3	0	0	0
3.5	18	2	3	0	22	0	1	0	0	0
4.5	39	1	3	0	31	0	11	0	0	0
5.5	40	0	3	0	39	1	10	0	2	0
6.5	54	0	6	0	36	0	8	0	1	0
7.5	72	0	11	0	55	2	12	0	1	0
8.5	126	2	9	1	54	3	14	0	2	0
9.5	83	2	7	0	34	0	10	0	3	2
10.5	70	7	6	0	23	3	2	0	3	0
11.5	56	2	8	0	18	0	3	0	0	1
12.5	35	0	7	1	12	0	5	0	1	1
13.5	51	2	5	0	21	2	5	0	1	0
14.5	42	0	4	0	21	1	5	0	2	1

Mid-Depth (cm)	Cassidulina reniforme	Cibicidoides wuellerstorfi	Cibicidoides pseudogerianus	Cibicidoides spp.	Cushmanina quadralata	Elphidium clavatum	Elphidium selseyense	Eubuliminella exilis	Fissurina / Parafissurina spp.	Globobulimina auriculata
0.25	1	0	0	0	0	0	0	12	0	0
0.75	0	0	0	0	0	0	0	9	1	0
1.5	0	0	0	0	0	0	0	21	1	0
2.5	2	0	1	0	0	0	0	14	1	0
3.5	4	0	1	0	0	0	0	10	0	0
4.5	10	0	1	0	0	0	0	16	2	0
5.5	1	0	1	0	0	0	0	6	1	0
6.5	3	0	0	0	0	0	0	7	2	0
7.5	7	0	1	0	0	0	0	16	4	0
8.5	16	0	2	0	0	0	0	14	2	0
9.5	13	0	3	0	2	0	0	8	4	0
10.5	5	0	3	0	1	0	0	5	1	0
11.5	8	0	2	0	0	0	0	5	4	0
12.5	7	0	2	0	0	0	0	6	4	0
13.5	8	0	2	0	0	0	0	4	4	0
14.5	10	0	1	0	0	0	0	7	2	0

Mid-Depth (cm)	Gyroidina lamarckiana	Islandiella islandica	Islandiella norcrossi	Lagena gracilima	Lagena hispidula	Lagena mollis	Lagena nebulosa	Lenticulina gibba	Miliolinella subrotunda	Nonionellina labradorica
0.25	0	0	0	0	0	0	0	0	0	0
0.75	1	0	0	0	0	0	0	0	0	0
1.5	2	0	0	0	0	0	0	0	0	0
2.5	1	0	0	0	0	0	0	0	0	2
3.5	1	0	0	0	0	0	0	0	0	0
4.5	5	0	0	0	0	0	0	1	0	0
5.5	9	0	0	0	0	0	0	1	0	0
6.5	8	0	0	0	0	0	0	1	0	3
7.5	17	0	0	2	0	0	0	1	0	1
8.5	8	0	0	0	0	0	0	2	0	1
9.5	6	0	0	0	0	0	0	2	1	1
10.5	5	0	0	0	0	0	0	0	2	1
11.5	4	0	0	0	2	0	0	0	0	0
12.5	5	0	0	3	0	1	0	0	0	2
13.5	7	0	0	0	0	0	0	0	2	3
14.5	3	0	0	0	0	0	0	0	0	0

Mid-Depth (cm)	Nonionoides turgidus	Oolina margaritae	Oridorsalis tenerusus	Paracassidulina neocarinata	Polymorphinidae	Pullenia osloensis	Pyrgo williamsoni	Quinqueloculina seminulum	Sagrina subspinescens	Stainforthia concava
0.25	0	0	0	0	23	14	0	0	2	0
0.75	0	0	0	0	18	6	0	0	1	0
1.5	0	0	0	0	10	8	0	0	0	1
2.5	1	0	0	0	9	30	0	0	1	3
3.5	0	0	0	0	0	21	0	0	1	1
4.5	0	0	0	2	3	43	0	0	1	1
5.5	0	0	0	3	4	32	0	1	0	1
6.5	2	0	0	1	4	50	0	1	3	2
7.5	2	0	0	5	4	70	0	1	3	3
8.5	4	0	3	5	14	105	0	5	4	6
9.5	0	0	4	5	6	71	0	3	1	1
10.5	1	0	6	4	2	69	0	4	3	2
11.5	2	0	3	1	10	79	0	2	5	7
12.5	0	0	1	2	8	47	1	1	1	2
13.5	4	0	1	1	10	60	1	1	1	2
14.5	0	0	0	1	7	52	1	2	0	3

Mid-Depth (cm)	Stainforthia fusiformis	Triloculina trigonula	Triloculina trihedra	Valvulineria arctica	Agglutinated	Total 63 – 106 µm
0.25	0	0	0	0	0	86
0.75	0	0	0	0	0	49
1.5	1	0	0	0	0	68
2.5	0	0	0	0	0	135
3.5	1	0	0	3	0	89
4.5	0	0	0	6	0	176
5.5	0	0	0	4	0	159
6.5	0	0	0	2	0	194
7.5	0	0	0	7	0	297
8.5	0	0	0	15	0	417
9.5	0	0	0	18	0	290
10.5	0	1	0	14	0	243
11.5	0	1	0	5	0	228
12.5	0	2	0	13	0	170
13.5	0	0	0	9	0	207
14.5	0	1	2	8	0	176

STATION 16

Mid-Depth (cm)	Alabaminella weddelensis	Astrononion gallowayi	Bolivinellina pseudopunctata	Brizalina subaenarensis	Buccella frigida	Bulimina marginata	Cassidulina neoteretis	Cassidulina leavigata and obtuosa	Cassidulina reniforme	Cibicidoides spp.
0.25	1	0	0	0	0	0	0	0	0	0
0.75	0	0	0	1	0	0	0	0	0	0
1.5	0	0	0	1	0	0	0	0	0	0
2.5	2	0	0	1	0	1	0	0	0	2
3.5	11	0	1	2	0	0	0	0	0	1
4.5	9	0	0	2	0	4	1	0	0	1
5.5	13	0	2	0	0	0	0	0	0	0
6.5	2	0	0	1	0	2	1	0	0	0
7.5	9	0	2	3	0	3	3	1	0	0
8.5	22	0	0	4	1	1	1	0	0	1
9.5	9	0	0	3	3	2	1	0	1	0
10.5	6	0	0	0	2	4	1	1	0	0
11.5	6	0	1	1	2	2	1	0	1	0
12.5	3	0	1	0	0	1	1	0	1	0
13.5	7	0	1	0	1	1	0	0	0	0
14.5	27	0	1	3	2	3	1	0	0	0
15.5	13	0	1	6	1	1	1	0	0	0
16.5	9	0	0	5	1	3	0	0	0	0
17.5	14	1	5	6	3	5	0	0	0	0
18.5	24	0	1	3	1	6	0	0	0	0
19.5	17	1	2	2	3	3	1	0	1	0

Mid-Depth (cm)	Elphidium clavatum	Elphidium selseyense	Eubuliminella exilis	Fissurina / Parafissurina spp.	Glandulina laevigata	Globobulimina auriculata	Globobulimina turgida	Lagena gracilima	Lagena mollis	Lagena nebulosa
0.25	0	0	2	0	0	0	0	0	0	0
0.75	0	0	6	0	0	0	0	0	0	0
1.5	0	0	11	0	0	0	0	0	0	0
2.5	0	0	5	0	0	0	0	0	0	0
3.5	0	0	8	1	1	1	0	0	0	0
4.5	1	0	9	1	1	0	0	0	2	0
5.5	1	0	11	3	1	0	0	1	0	0
6.5	1	0	9	2	0	0	0	0	0	0
7.5	3	7	12	0	0	0	0	0	0	0
8.5	5	5	10	3	2	0	0	0	0	0
9.5	2	1	11	1	0	1	0	0	1	0
10.5	2	1	12	5	2	0	0	0	1	0
11.5	6	0	13	6	1	0	0	0	1	0
12.5	2	1	10	4	0	0	0	0	0	0
13.5	6	0	7	3	0	0	0	0	0	0
14.5	9	1	8	6	0	1	0	0	0	0
15.5	6	5	11	0	0	0	0	0	0	0
16.5	4	1	5	1	0	0	0	0	0	0
17.5	9	0	8	2	0	0	0	1	3	0
18.5	8	0	10	1	1	0	0	0	0	0
19.5	7	0	5	0	0	0	0	0	2	0

Mid-Depth (cm)	Lenticulina gibba	Miliolinella subrotunda	Nonionellina labradorica	Nonionoides turgidus	Oolina hexagona	Oridorsalis tenerusus	Paracassidulina neocarinata	Polymorphinidae	Pullenia osloensis	Pyrgo williamsoni
0.25	0	0	0	0	0	0	0	0	0	0
0.75	0	0	0	0	0	0	0	0	0	0
1.5	0	0	0	0	0	0	0	0	0	0
2.5	0	0	0	0	0	0	1	0	2	0
3.5	0	0	0	0	0	0	3	3	10	0
4.5	0	0	0	0	0	1	3	1	7	0
5.5	0	0	0	0	0	0	5	0	13	0
6.5	0	0	0	0	0	0	2	0	1	0
7.5	0	1	0	0	0	1	4	0	9	3
8.5	2	0	1	0	0	1	3	1	22	1
9.5	2	0	2	0	0	0	2	1	9	1
10.5	0	0	0	1	0	1	3	0	6	3
11.5	0	0	1	0	0	1	2	0	6	1
12.5	0	0	1	0	0	1	1	2	25	0
13.5	0	0	0	0	0	1	0	1	7	1
14.5	0	0	5	1	0	1	2	1	27	3
15.5	0	0	1	0	0	1	1	1	13	1
16.5	1	0	1	0	0	1	1	0	2	3
17.5	0	0	2	0	0	2	3	0	14	2
18.5	2	1	2	1	0	2	2	0	24	6
19.5	0	0	1	0	0	1	3	0	17	1

Mid-Depth (cm)	Quinqueloculina seminulum	Reussoolina laevis	Sagrina subspinescens	Spiroloculina sp. A	Stainforthia concava	Triloculina trigonula	Valvulineria arctica	Agglutinated	Total 63 – 106 µm
0.25	0	0	0	0	0	0	0	41	44
0.75	0	0	0	0	3	0	0	25	35
1.5	0	0	1	0	0	0	0	9	22
2.5	0	0	0	0	0	0	1	5	20
3.5	0	0	1	0	0	0	0	8	51
4.5	0	2	0	0	0	0	1	3	49
5.5	0	1	0	0	1	1	0	0	53
6.5	0	0	0	0	0	0	0	1	22
7.5	0	0	3	0	0	1	0	0	65
8.5	2	0	0	0	0	1	1	0	90
9.5	2	0	0	0	0	0	0	0	55
10.5	0	0	0	0	0	0	2	0	53
11.5	3	1	0	0	5	1	3	0	65
12.5	2	0	0	0	0	0	4	0	60
13.5	2	2	2	0	3	0	0	0	45
14.5	7	0	1	0	1	0	0	0	111
15.5	0	0	0	0	0	0	6	0	69
16.5	3	0	1	1	0	0	1	0	44
17.5	6	0	0	0	2	0	3	0	91
18.5	7	0	2	0	0	0	5	0	109
19.5	6	1	1	0	3	1	4	0	83

ANNEXE D : MATÉRIEL SUPPLÉMENTAIRE

Tableau S1   Concentrations d'oxygène dissous (DO) à 250 à 355 m de profondeur d'eau dans l'EMSL selon sur les données extraites en 2018 de la base de données BioChem, mise à disposition par le ministère des Pêches et des Océans Canada, et une compilation des données acquises sur le *R/V Coriolis II* (étendu de Gilbert et al., 2005 ; Jutras et al., 2020a)

Age (CE)	DO at station 23 (µM)		DO at station 21 (µM)	DO at station 18.5 (µM)	DO at station 16 (µM)
2018	50.0	± 0.8	58.2	95	153.2
2017	57.8	± 0.2	63.4	91.7	
2016			69.4	108	
2015	56.7	± 0.4			
2014	63.5	± 0.4			
2013				85.6	
2012	62.7	± 0.2			
2011	60.4	± 0.5			
2010			67.3	124.7	196.6
2009	64.3		71.2		
2008				96.7	159.6
2007	56.6	± 0.5			
2006	60.9	± 0.4			
2005	63		80.7	155	
2003	50.5		81.6	109.9	116
2002	59.8	± 5.4			

|		
1990	75	± 4.8
1987	58.7	± 3.8
1984	66.8	
1975	104.3	± 10
1974	103.8	
1973	100	± 2.4
1972	109.1	± 13.5
1971	117.3	
1970	111	
1964	94.2	
1961	80.8	
1935	126	± 0.4
1934	136.5	± 0.6
1933	128.8	± 0.3
1932	107.7	± 0.35

Tableau S2   Scores des axes RDA 1 et 2 des taxons de foraminifères benthiques à la station 23 avec l'oxygène dissous, la température, le rapport molaire du carbone organique à l'azote total (C:N) et le $\delta^{13}C$ du carbone organique comme variables environnementales. Les axes RDA 1 et 2 expliquent respectivement 52% et 11% de la variance. Les analyses multivariées ont été réalisées à l'aide du logiciel CANOCO 5 (Ter Braak & Šmilauer, 2012)

Taxa	RDA axis 1 scores	RDA axis 2 scores
Brizalina subaenariensis	−0.7840	0.2260
Eubuliminella exilis	−0.8171	−0.1111
Globobulimina auriculata	−0.3342	−0.5978
Nonionellina labradorica	0.4084	−0.1653
Bulimina marginata	0.8289	0.3168
Pullenia osloensis	0.9471	−0.0589
Cassidulina reniforme	0.8410	−0.0558
Elphidium spp.	0.4402	0.4404
Stainforthia concava	0.7376	0.3239
Lagena/Oolina spp.	0.8285	0.3057
Islandiella norcrossi	0.6101	0.2609
Sagrina subspinesens	0.7308	0.2475
Gyroidina lamarckiana	0.6911	0.2279
Polymorphinidae	0.6582	0.1852
Bolivinella pseudopunctata	0.5443	0.4826
Alabaminella weddelensis	0.3085	0.0949
Valvulineria arctica	0.7191	0.0619
Fissurina / Parafissurina spp.	0.0203	−0.5087
Quinqueloculina seminulum	−0.0428	0.3540
Pyrgo williamsoni	0.7261	0.1058

Environmental variables	RDA axis 1 scores	RDA axis 2 scores
Dissolved oxygen	0.9690	0.0542
Temperature	−0.6241	−0.2804
$\delta^{13}C$	−0.4979	−0.6320
C:N	0.6673	0.6703
Environmental variables	Correlation with RDA axis 1	Correlation with RDA axis 2
Dissolved oxygen	0.9024	0.0342
Temperature	−0.5812	−0.1768
$\delta^{13}C$	−0.4637	−0.3984
C:N	0.6214	0.4225

Figure S3   *Plum* age-depth models for A) station 23, B) station 21, C) station 18.5, and D) station 16. The blue rectangles represent the ^{210}Pb activity (Bq kg^{-1}). The red line represents the mean model. The grey dashed lines are the 95% confidence intervals. The purple rectangles represent the ^{226}Ra activity (Bq kg^{-1}). The priors (green lines) and posteriors (grey plots) for each model are shown in the mini plots above the age-depth models. Based on estimated sedimentation rates, the prior parameters corresponding to accumulation rates (*acc.mean*) were set to 1.4 a cm^{-1}, 2 a cm^{-1}, 3 a cm^{-1}, and 10 a cm^{-1} for stations 23, 21, 18.5 and 16, respectively
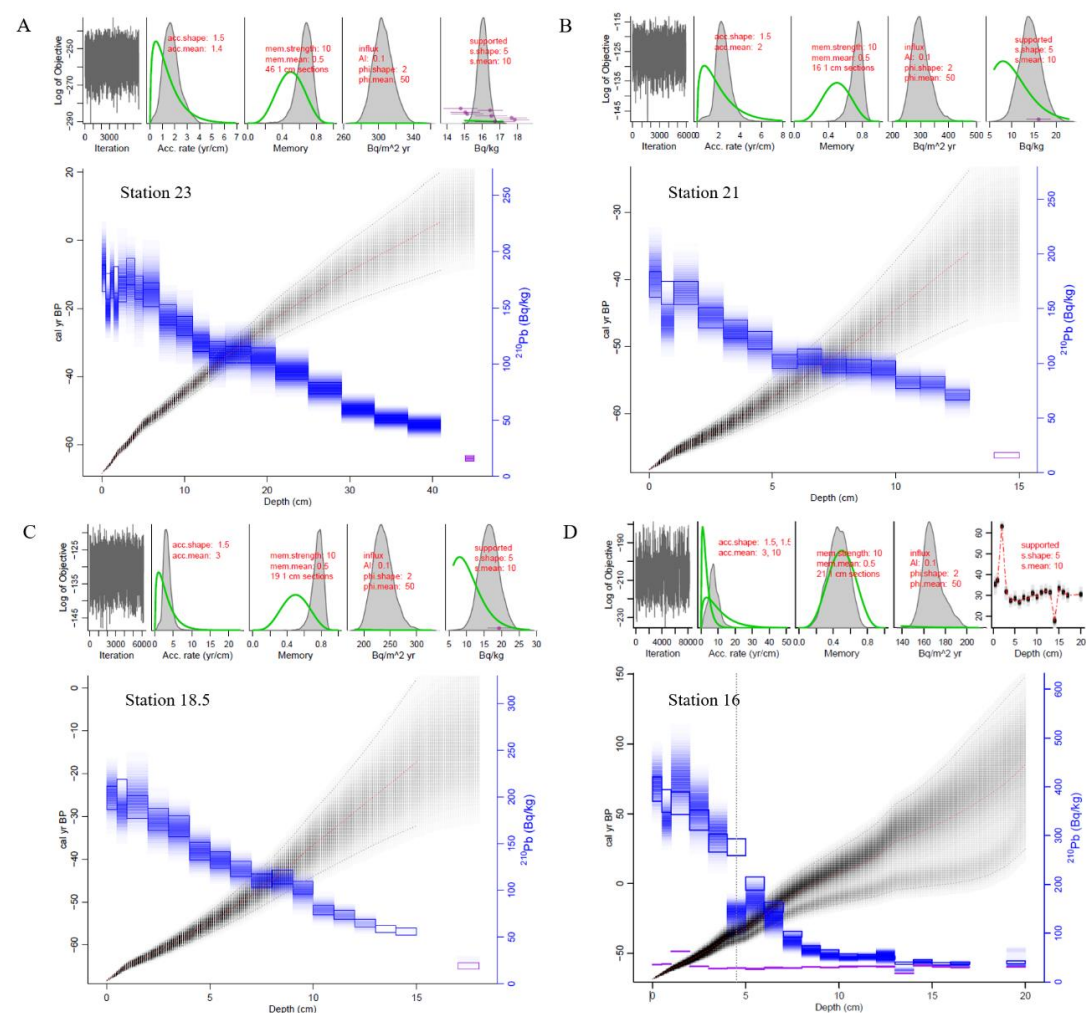
BIBLIOGRAPHIE GÉNÉRALE

Belley, R., Archambault. P., Sundby, B., Gilbert, F., and Gagnon, J.-M. (2010). Effects of hypoxia on benthic macrofauna and bioturbation in the Estuary and Gulf of St. Lawrence, Canada. *Continental Shelf Research, v. 30*, p.1302–1313.

Bernhard, J. M., Sen Gupta, B. K. and Borne, P. F. (1997). Benthic foraminiferal proxy to estimate dysoxic bottom-water oxygen concentrations; Santa Barbara Basin, U.S. Pacific continental margin. *Journal of Foraminiferal Research, v. 27*, p. 301–310. doi: 10.2113/gsjfr.27.4.301

Breitburg, D. (2002). Effects of hypoxia, and the balance between hypoxia and enrichment, on coastal fishes and fisheries: *Estuaries*, *25*, 767–781. https://doi.org/10.1007/BF02804904

Brüchert, V., Pérez, M. E. and Lange, C. B. (2000). Coupled primary production, benthic foraminiferal assemblage, and sulfur diagenesis in organic-rich sediments of the Benguela upwelling system. *Marine Geology, v. 163*, p. 27–40. https://doi.org/10.1016/S0025-3227(99)00099-7

D'Amours, D. (1993). The distribution of cod (*Qadus morhua*) in relation to temperature and oxygen level in the Gulf of St. Lawrence. *Fisheries Oceanography*, *2*(1), 24–29. https://doi.org/10.1111/j.1365-2419.1993.tb00009.x

Dupont-Prinet, A., Pillet, M., Chabot, D., Hansen, T., Tremblay, R. et Audet, C. (2013). Northern shrimp (*Pandalus borealis*) oxygen consumption and metabolic enzyme activities are severely constrained by hypoxia in the Estuary and Gulf of St. Lawrence. *Journal of Experimental Marine Biology and Ecology*, *448*, 298–307. https://doi.org/10.1016/j.jembe.2013.07.019

Erdem, Z., Schönfeld, J., Rathburn, A.E., Pérez, M.-E., Cardich, J., Glock, N. (2020). Bottom-water deoxygenation at the Peruvian margin during the last deglaciation recorded by benthic foraminifera. *Biogeosciences v. 17*, p. 3165–3182. doi:10.5194/bg-17-3165-2020

Genovesi, L., de Vernal, A., Thibodeau, B., Hillaire-Marcel, C., Mucci, A. et Gilbert, D. (2011) Recent changes in bottom water oxygenation and temperature in the Gulf of St. Lawrence. Micropaleontological and geochemical evidence. *Limnology and Oceanography*, *56*(4), 1319–1329.

Gilbert, D., Sundby, B., Gobeil, C., Mucci, A. and Tremblay, G. H. (2005). A seventy-two-year record of diminishing deep-water oxygen in the St. Lawrence estuary: The northwest Atlantic connection. *Limnology and Oceanography, v. 50*, p. 1654–1666.

Gilbert, D., Chabot, D., Archambault, P., Rondeau, B., Hébert, S. (2007). Appauvrissement en oxygène dans les eaux profondes du Saint-Laurent marin Causes possibles et impacts écologiques. *Naturaliste Canadien v.131*: p. 67–75.

Hoogakker, B. A. A., Lu, Z., Umling, N., Jones, L., Zhou, X., Rickaby, R. E. M., Thunell, R., Cartapanis, O., Galbraith, E. (2018) Glacial expansion of oxygen-depleted seawater in the eastern tropical Pacific. *Nature v. 562*, p. 410–413. doi:10.1038/s41586-018-0589-x

Hooper, K. (1975). Foraminiferal ecology and associated sediments of the lower St. Lawrence Estuary. *Journal of Foraminiferal Research*, *5*(3), 218–238. doi: 10.2113/gsjfr.5.3.218

Jorissen, F. J., Fontanier, C. et Thomas, E. (2007). Chapter Seven Paleoceanographical Proxies Based on Deep-Sea Benthic Foraminiferal Assemblage Characteristics. Dans C. Hillaire–Marcel et A. De Vernal (dir.), *Developments in Marine Geology* (vol. 1, p. 263–325). Elsevier.

Jutras, M., Dufour, C. O., Mucci, A., Cyr, F. et Gilbert, D. (2020a). Temporal changes in the causes of the observed oxygen decline in the St. Lawrence Estuary. *Journal of Geophysical Research: Oceans*, *125*, e2020JC016577. https://doi.org/10.1029/2020JC016577

Jutras, M., Mucci, A., Sundby, B., Gratton, Y. et Katsev, S. (2020b). Nutrient cycling in the Lower St. Lawrence Estuary: Response to environmental perturbations. *Estuarine, Coastal and Shelf Science*, *239*, 106715. doi: https://doi.org/10.1016/j.ecss.2020.106715

Jutras, M., Mucci, A., Chaillou, G., Nesbitt, W. A., and Wallace, D. W. R. (2022). Temporal and spatial evolution of bottom-water hypoxia in the Estuary and Gulf of St. Lawrence. *Biogeoscience Discussion*, https://doi.org/10.5194/egusphere-2022-1090.

Kaiho, K. (1994). Benthic foraminiferal dissolved-oxygen index and dissolved-oxygen levels in the modern ocean, Geology, v. 22, 719–722. doi: 10.1130/0091-7613(1994)022<0719:Bfdoia>2.3.Co;2

Karlsen, A. W., Cronin, T. M., Ishman, S. E., Willard, D. A., Kerhin, R., Holmes, C. W. et Marot, M. (2000). Historical trends in Chesapeake Bay dissolved oxygen based on benthic foraminifera from sediment cores. *Estuaries*, *23*(4), p. 488–508. doi: 10.2307/1353141

Loubere, P. (1994). Quantitative estimation of surface ocean productivity and bottom water oxygen concentration using benthic foraminifera. *Paleoceanography, 9*(5), 723–737. doi: https://doi.org/10.1029/94PA01624

Murray, J. W. (2006). Ecology and applications of benthic foraminifera. *Cambridge University Press*, Cambridge, 426 p.

Ohkushi, K., Kennett, J. P., Zeleski, C. M., Moffitt, S. E., Hill, T. M., Robert, C., Beaufort, L., and Behl, R. J. (2013). Quantified intermediate water oxygenation history of the NE Pacific: A new benthic foraminiferal record from Santa Barbara basin. *Paleoceanography, v. 28*, p. 453– 467.

Osterman, L. E. (2003). Benthic foraminifers from the continental shelf and slope of the Gulf of Mexico: an indicator of shelf hypoxia. *Estuarine, Coastal and Shelf Science, 58*(1), 17–35. https://doi.org/10.1016/S0272-7714(02)00352-9

Platon, E., Gupta, B. K. S., Rabalais, N. N. et Turner, R. E. (2005). Effect of seasonal hypoxia on the benthic foraminiferal community of the Louisiana inner continental shelf: The 20th century record. *Marine Micropaleontology, 54*(3–4), 263–283. https://doi.org/10.1016/j.marmicro.2004.12.004

Rodrigues, C. G. et Hooper, K. (1982). Recent benthonic foraminiferal associations from offshore environments in the Gulf of St. Lawrence. *Journal of Foraminiferal Research, 12*(4), 327–352. doi: 10.2113/gsjfr.12.4.327

Sen Gupta, B.K. (1999). Modern foraminifera. *Kluwer Academic Publishers*, Baton Rouge, 371 p.

Sen Gupta, B. K. et Machain-Castillo, M. L. (1993). Benthic foraminifera in oxygen-poor habitats. *Marine Micropaleontology, 20*(3), 183–201. doi: https://doi.org/10.1016/0377-8398(93)90032-S

Tetard, M., Beaufort, L. and Licari, L. (2017). A new optical method for automated pore analysis on benthic foraminifera. *Marine Micropaleontology, v. 136*, p.30–36.

Tetard, M., Ovsepyan, E. and Licari, L. (2021a). *Eubuliminella tenuata* as a new proxy for quantifying past bottom water oxygenation. *Marine Micropaleontology, v. 166*, p. 102016. doi: https://doi.org/10.1016/j.marmicro.2021.102016

Tetard, M., Licari, L., Ovsepyan, E., Tachikawa, K., Beaufort, L. (2021b). Toward a global calibration for quantifying past oxygenation in oxygen minimum zones using benthic Foraminifera. *Biogeosciences, v. 18*, p. 2827–2841. doi:10.5194/bg-18-2827-2021

Thibodeau, B., de Vernal, A. and Mucci, A. (2006). Recent eutrophication and consequent hypoxia in the bottom waters of the Lower St. Lawrence Estuary: Micropaleontological and geochemical evidence. *Marine Geology, v. 231*, p. 37–50.

Thibodeau, B., Lehmann, M. F., Kowarzyk, J., Mucci, A., Gélinas, Y., Gilbert, D., Maranger, R. and Alkhatib, M. (2010). Benthic nutrient fluxes along the Laurentian Channel: Impacts on the N budget of the St. Lawrence marine system. *Estuarine, Coastal and Shelf Science, v. 90,* p. 195–205. doi: https://doi.org/10.1016/j.ecss.2010.08.015

Thibodeau, B., de Vernal, A. and Limoges, A. (2013). Low oxygen events in the Laurentian Channel during the Holocene. *Marine Geology, v. 346,* p. 183–191. doi: https://doi.org/10.1016/j.margeo.2013.08.004

Thibodeau, B., Not, C., Zhu, J., Schmittner, A., Noone, D., Tabor, C., Zhang, J. and Liu, Z. (2018). Last century warming over the Canadian Atlantic shelves linked to weak Atlantic meridional overturning circulation. *Geophysical Research Letters, v. 45*, p. 12,376– 12,385. https://doi.org/10.1029/2018GL080083